Ofioliti An International Journal on Ophiolites and Modern Oceanic Lithosphere

JOURNAL PRE-PROOF

EXTENSION OF THE BERIT SUTURE ZONE TO EASTERNMOST TÜRKIYE (EAST OF LAKE VAN): EVIDENCE FROM AN UPPER CRETACEOUS INTRA-OCEANIC ARC, SUPRA-SUBDUCTION ZONE OPHIOLITES, AND PALAEOZOIC-CENOZOIC SEDIMENTARY SUCCESSIONS

To appear in OFIOLITI 52, 1 (2027)
DOI: https://doi.org/10.4454/ofioliti.v52i1.594

Received date: 20 April, 2026
Accepted date: 23 July, 2026
First published online: 26 September, 2026

EXTENSION OF THE BERIT SUTURE ZONE TO EASTERNMOST TÜRKIYE (EAST OF LAKE VAN): EVIDENCE FROM AN UPPER CRETACEOUS INTRA-OCEANIC ARC, SUPRA-SUBDUCTION ZONE OPHIOLITES, AND PALAEOZOIC-CENOZOIC SEDIMENTARY SUCCESSIONS

Alastair H.F. Robertson*✉, Osman Parlak**✉, Kemal Taslı***

[*]School of GeoSciences, University of Edinburgh, Grant Institute, James Hutton Road, Edinburgh, EH9 3FE, UK
[**]Çukurova Üniversitesi, Jeoloji Mühendisliği Bölümü, 01330 Balcalı, Adana, Türkiye
[***]Mersin Üniversitesi, Jeoloji Mühendisliği Bölümü, 33100 Mersin, Türkiye

✉Corresponding authors, E-mail addresses: Alastair.Robertson@ed.ac.uk; parlak@cu.edu.tr

Keywords: Easternmost Türkiye, Van area, Berit suture, oceanic arc, SSZ ophiolite, Cenozoic cover, compression events

ABSTRACT

This paper discusses and interprets the important but little studied eastward extension of the regionally important Berit Suture Zone that extends across eastern Türkiye into Iran (>500km). Fragmentary Upper Cretaceous ophiolites, oceanic island arc units and accretionary melange, east of Lake Van, are keys to an understanding of the Berit Suture Zone in this area. Field and geochemical evidence suggest that a dismembered ophiolite (Mehmetalan ophiolite) in the study area, mainly depleted mantle harzburgite, dunite and cumulate gabbro, formed in an Upper Cretaceous fore-arc setting. Cross-cutting alkaline diabase dykes in one of the ophiolite fragments hints at plume involvement. The volcanic arc, part of the regional Yüksekova Complex, is dominated by variably evolved tholeiitic, calc-alkaline and alkaline volcanics that erupted in an open-ocean setting, together with minor granodioritic intrusives. Intercalated pelagic carbonates are dated here as Campanian-Maastrichtian (locally late Maastrichtian) based on planktic foraminifera. The arc-related volcanics display two geochemical trends: one is typical of variably evolved basic-felsic oceanic arc volcanism; the other is alkaline and could represent escape of relatively enriched upper mantle through a slab rupture or alternatively plume involvement in the SSZ magmatism. A dismembered Palaeozoic-Mesozoic platform succession in the area can be correlated with the Malatya-Keban (Tauride) platform >300 km to the west. The deposition and deformation of the sedimentary cover units, of Late Palaeocene-Middle Eocene and also of Oligocene-Early Miocene age, help to constrain the timing of deformation. Three main phases of southward-directed compression, thrusting and consequent subaerial erosion are recognised: latest Cretaceous, Late Eocene and Mid-Late Miocene. This was followed by plateau uplift, strike-slip/transpression and westward ‘tectonic escape’. The proposed tectonic model correlates the various units east of Lake Van with the development of the Berit Ocean between the Malatya-Keban platform to the north and the Pütürge and Bitlis metamorphic units generally to the south. Differences, however, include the absence of

exposed Bitlis continental crust to the south, the lack of significant Eocene volcanism, thrust emplacement farther south, and a more complex and variable deformation history.

INTRODUCTION

Many suture zones worldwide are characterised by the development of subduction-accretion complexes. Some accretionary complexes cover vast areas, for example the Central Asian Orogenic Belt (Windley et al., 2007), the Western Kunlun Orogen (Dong et al., 2008), and the Appalachians of Newfoundland (Hatcher, 2010). In such suture zones, the tectono-stratigraphy is not anchored to any exposed reference point (e.g., basement or continent), and therefore the geological development must be interpreted based on the internal tectonostratigraphy that may be variable and complex. Here, we discus and interpret the eastward extension of the regionally important Berit Suture Zone in easternmost Türkiye. The Berit Suture Zone forms a large of part of the East Anatolian Accretionary Complex, which separates Eurasia and Gondwana-related continental units in easternmost Türkiye (Şengör et al., 2008; Keskin, 2005; Topuz et al., 2013), specifically the area extending from Van Gölü (Lake Van) to beyond the Iranian border (Figs. 1,2). This large area (c. 8000 km^2) is topographically varied, dominated by approximately east-west trending hills and mountains (e.g., SE of Van city) with similar trending valleys (e.g., east and west of Erçek Gölü (Lake Erçek; Fig. 2). Parts of the area, mainly in the north, are covered by Upper Miocene-recent volcanics and sediments, restricting older exposures to variable-sized, isolated outcrops (Fig. 2). The whole region is seismically active in a compressional and left-lateral strike-slip (transpressional) mode related to the westward tectonic 'escape' of Anatolia from the African-Eurasia plate collision zone (Koçyiğit et al., 2001; Koçyiğit, 2013; Görur et al., 2015; Özalp et al., 2016; Çukur et al., 2017). This area has mainly been geologically mapped at 1:500,000 and 1:250,000 scales by the Maden Tetkik ve Arama Genel Müdürlüğü, and 1:100,000 scale maps and reports are published for four quadrangles east of Van city (K50, K51, K52, L51, L52; Şenel et al., 1984; Şenel, 1987; Sümengen, 2008a,b,c). However, geological information on the pre-Plio-Quaternary remains sparse, other than for several petrological and geochemical studies of intrusive ophiolitic and arc-type volcanic rocks.

The main objectives of this paper are to summarise and interpret the eastward extension of the Berit Suture Zone in easternmost Türkiye, east of Lake Van, in its regional tectonic context. The specific aims are: (1) to present new geochemical and microfossil data concerning the Yüksekova Complex, a regionally important Upper Cretaceous arc-related unit; (2) to summarise and interpret the tectono-stratigraphic and structural development, including the formation and emplacement of Upper Cretaceous oceanic volcanic arc and ophiolitic units; (3) to consider and reconstruct Palaeozoic-Upper Cretaceous dismembered platform-related lithologies; (4) to provide new sedimentological and microfossil evidence for Palaeocene to Lower Miocene sedimentary successions that are also important to understand the timing of deformation; and (5) to present a new tectonic model for the area in the context of closure of the Mesozoic Berit Ocean.

METHODS

During September 2024, selected outcrops were studied, together with reconnaissance mainly between Lake Van and the town of Özalp c. 45 km to the east (Fig. 2). Particular attention was paid to the contact relations of the main tectono-stratigraphical units, the internal structural relationship, the Upper Cretaceous volcanics and the Palaeocene-Miocene sedimentary rocks.

Samples of volcanic rocks from the Upper Cretaceous Yüksekova Complex were studied petrologically at the Department of Geological Engineering, Çukurova University, Adana. The published data base of 25 chemical analyses was supplemented by analysis of four samples of relatively non-evolved aphyric volcanic rocks, aiding comparisons with modern and ancient counterparts. One sample of hitherto unmapped basaltic rock (YU24-97) was also analysed from a mapped Triassic exposure.

The volcanic rocks were analysed for major elements and trace elements including rare earth elements (REEs) at ALS Lab in Ireland. Major element concentrations were determined from a $LiBO_2$ fusion by inductively coupled plasma mass spectrometry (ICP-AES), by using 2g of sample pulp. Trace element contents were determined from a $LiBO_2$ fusion by ICP-MS, by using 2g of sample pulp. Major and trace element compositions of the analysed volcanic rocks were calibrated against international reference materials (SY-5, OREAS 102a, MRGeo08, AMIS0362, AMIS0353, AMIS0304, AMIS0356 and REE-1).

In addition, thin sections of mainly Upper Cretaceous and Palaeogene sedimentary rocks were studied using an optical microscope at the School of GeoSciences, University of Edinburgh. Samples from Upper Cretaceous to Miocene sedimentary units were observed in thin sections at Mersin University, allowing microfossils to be dated.

The new data were synthesised with existing information and used to help understand the geological development of easternmost Türkiye, especially the eastward extension of the Berit Ocean.

The timescale of Cohen et al. (2021) is used in this paper.

REGIONAL GEOLOGICAL SETTING AND TECTONO-STRATIGRAPHIC UNITS

The study area east of Lake Van exposes six tectono-stratigraphical units, as shown on the simplified regional map (Fig. 2), and on more detailed geological maps of two selected areas, one within the study area (Fig. 3), and one farther south from the literature (Fig. 4): (1) extrusive igneous rocks, subordinate intrusive rocks, and associated deep-sea sedimentary rocks of the Yüksekova Complex; (2) dismembered Upper Cretaceous ophiolite and related ophiolitic melange, known as the Mehmetalan ophiolite; (3) ophiolite-related melange, mixed ophiolitic and non-ophiolitic sedimentary and igneous material, here termed Bakışık Melange; (4) Palaeozoic-Mesozoic dismembered mainly sedimentary succession, referred to here as the Palaeozoic-Mesozoic unit; (5) Upper Paleogene-Lower Eocene shallow to deeper water sediments (Toprakkale and Yücelendere formations, respectively); (6) Upper Oligocene-Lower Miocene shallow-water carbonate and terrigenous clastic successions (Adilcevaz and Van formations, respectively (Şenel et al., 1984; Şenel, 1987; Sümengen, 2008a,b,c).

The East Anatolian Accretionary Complex including the study area east of Lake Van is bordered to the north by the Upper Cretaceous Pontide continental margin arc and to the south by the Bitlis and Pütürge continental units (Fig. 1). Eastwards, in Iranian territory, the outcrop merges with the Sanandaj-Sirjan Zone (Juteau, 2004; Saccani et al., 2013; Moghadam et al., 2019; Haji et al., 2020) and the Inner Zagros ophiolite belt (Saccani et al., 2013; Haji et al., 2020). In Iran, the Khoy ophiolitic complex includes basalts of E-MORB to N-MORB composition (Hassanipak et al., 2000; Ghazi et al., 2003), and associated pelagic carbonates contain late Campanian and Middle-Late Eocene planktic foraminifera (Ghazi et al., 2003; Pessagno et al., 2005). These ophiolite-related rocks are, therefore, dissimilar to the Yüksekova Complex in several respects. Some other ophiolites farther east in Iran are of SSZ type and are likely to be more similar to the dismembered ophiolitic rocks in the present study area, although these are not discussed farther here.

North of the study area, additional accretionary units (MTA, 2011) relate to closure of the Mesozoic İzmir-Ankara-Erzincan Ocean (northern Neotethys) (Robertson et al., 2012, 2013). To the northwest of the study area, the accretionary complex is bordered by the continental Malatya-Keban unit (Perinçek and Kozlu, 1984; MTA, 2011). The outcrop to the south and southwest of this crustal unit is known as the Berit Suture Zone, which formed by closure of the Mesozoic Berit Ocean (Robertson et al., 2006, 2012, 2013, 2021), also known as the Amanos-Elazığ-Van Ocean (Göncüoğlu et al., 1997; Göncüoğlu, 2014) and the Alanya-Bitlis Ocean (Çetinkaplan et al., 2016). The Berit Suture Zone potentially correlates with the study area east of Lake Van (see Discussion). The Berit Suture Zone is bordered to the south by the Bitlis and Pütürge continental units (Göncüoğlu and Turhan, 1984; MTA, 2011). Related to continental collision, much of area of the East Anatolian Accretionary Complex is interpreted to be underlain by continental crust (Topuz et al., 2017; Yılmaz et al., 2023), although this does not affect the interpretation of the pre-collision tectonic units in the area as an Upper Cretaceous accretionary complex.

Farther south, additional accretionary units relate to the closure of the Mesozoic Southern Neotethys against the Arabian continent to the south (Fig.1), although this is outside the present scope.

Each of the six main units making up the study area east of Lake Van are summarised below.

Upper Cretaceous Yüksekova Complex

The Upper Cretaceous Yüksekova Complex is exposed widely across eastern Anatolia and extends into Iran within the Sanandaj-Sirjan zone (Figs. 2-4). The type area of the Yüksekova Complex is near Yüksekova town, c. 100 km south-southeast of Lake Van, where the succession is relatively intact, allowing recognition of a composite succession (Fig. 5). Equivalent lithologies are also exposed extensively 300 km farther west (Kovancılar-Elazığ-Maden area; Fig. 2), where they have been termed the Elazığ Magmatics, the Elazığ Magmatic Complex, or the Elazığ Magmatic unit (Bingöl 1984; Aktaş and Robertson, 1984, Beyarslan and Bingöl, 2000; Bingöl et al., 2018), after the regional city, Elazığ which is near some of the most extensive exposures. More recently the term Yüksekova Complex has been applied to the entire suite of Upper Cretaceous oceanic arc-related lithologies right across eastern Anatolia (Karaoğlan et al., 2013; Ural et al., 2015, 2021, 2022).

Within the study area, the Yüksekova Complex has several large outcrops; e.g., southeast and northeast of Çardak, east and southeast of Van city (Figs. 3, 4, 6a) and north and northeast of Lake Erçek, together with numerous scattered outcrops (Fig. 2). The complex is commonly cut by anastomosing strands of sheared serpentinite, typically up to tens of m thick and traceable laterally for 100s m to several km. During this study, it was found that some outcrops mapped as ophiolitic melange belong to the Yüksekova Complex, although the implied need for some remapping was beyond the scope of this research.

The Yüksekova Complex in the study area is typically dominated by massive and pillowed basaltic-andesitic to locally rhyo-dacitic lava flows (Figs. 6b-d), with lenticular intercalations of pinkish pelagic limestones (Fig. 6e). Excellent, easily accessible exposures were observed, for example, to the west and east of Çardak (Fig. 2). Individual lava flows are typically up to several tens of metres thick and include hyaloclastite, lava breccia (agglomerate), matrix-supported conglomerates (mass-flows) and thin (<c. 15 cm) layers of pale siliceous tuff. Interbedded pelagic limestones (Figs. 6b,e, 8a) are typically lenticular (< 10 m thick and 10-100s m long). Pelagic limestones have been mapped as thicker and more extensive in the far southeast near the Iranian border (Kandilli limestones) (Şenel et al., 1984

Şenel, 1987) (Fig. 4). Volcanogenic mudstone and sandstone turbidites are locally intercalated with the lavas (Fig. 6f). In thin section, the sandstones contain variable abundances of basic, intermediate and felsic composition lithoclasts, with common plagioclase, monocrystalline quartz and opaque mineral grains (Fig. 8b); ferromagnesian minerals, mostly clinopyroxene and olivine are sparse. Small gabbroic bodies (undated) are reported, mainly in the east near the Iranian border (Şenel et al., 1984; Şenel, 1987) although in places it is unclear which of these are intrusive into the Yüksekova Complex and which could be of ophiolitic origin. Small granitic intrusions are also locally exposed, for example northeast of Lake Erçek (GPS: 38S 379749E/4289900N). Near Çardak (GPS: 38S 419626E/4263891N), lavas of the Yüksekova Complex are cut by a small granitic intrusion. These lavas are hydrothermally altered and enriched in disseminated copper (Figs. 6g,7).

Petrography and geochemistry of volcanic rocks

The volcanic rocks of the Yüksekova Complex in the areas east of Van contain plagioclase and clinopyroxene phenocrysts and exhibit amygdaloidal, microlitic, porphyritic and subophitic textures (Fig. 9a–d). The clinopyroxene phenocrysts vary from euhedral to anhedral (Fig. 9a,c). The groundmass consists of plagioclase microlites and interstitial anhedral clinopyroxene (Fig. 9a-d). Plagioclase occurs both as phenocrysts (Fig. 9a-d) and microlites, and is commonly altered to albite, due to low-grade metamorphism or late-stage hydrothermal processes. Secondary mineral phases include calcite filling amygdales and chlorite within the groundmass (Fig. 9a,d).

Previously, 25 samples of volcanic rock were analysed for major, trace and rare earth elements from a relatively small area (c. 25 sq. km) in the vicinity of Gövelek, c. 20 km northeast of Van city (S of Erçek Lake) (Özdemir, 2016; Fig. 2). These samples fall into tholeiitic, calc-alkaline and alkaline categories. They show marked variations in Sr and Nd isotopic compositions, with the more radiogenic example coinciding with a calc-alkaline composition (Özdemir, 2016). Ar-Ar dating gave ages of 113 ± 3 Ma (Aptian-Albian boundary) for a tholeiitic volcanic, 66.5 ± 0.3 Ma (early Danian) for a calc-alkaline volcanic, and 44 ± 0.3 Ma (Lutetian) for an alkaline volcanic sample (Gövelek area). Also, seven lavas and two crosscutting dykes (one lamphrophyric) were analysed separately (Çolakoğlu et al., 2014) from another small area (c.15 sq. km.), located east of Erçek Lake. These lavas range from alkali basalts, to trachyandesite, to basanite, and to nephelinite. Inter-pillow lava pink pelagic carbonate contains late Maastrichtian planktic foraminifera (Çolakoğlu et al., 2014). These authors considered these lavas and dykes to be part of what they termed the Yüksekova melange, which they interpreted as part of a dismembered ophiolite, although they are instead correlated here with the Yüksekova Complex in view of similarities in composition and age (see Discussion).

During this study, four critically located lava samples were analysed from near Lake Gövelek (YU24-87), NE of Lake Erçek (YU24-103), near Çardak (YU24-115) and from southeast of Lake Van (YU24-130) (Table S2). The samples from near Çardak and from southeast of Lake Van are from areas without published analytical data.

The combined new and existing data (Çolakoğlu et al., 2014; Özdemir, 2016; this study) are plotted on lithology and petrogenetic diagrams in Figure 11a-h, together with analyses from the type area of the Yüksekova Complex, c. 100 km to the south (Robertson et al., 2026). On the lithology discrimination diagram (Fig. 11a), the majority of the samples of the present study and those of the Yüksekova Complex type area plot in the basalt-andesite/basaltic andesite, and rhyolite/dacite fields. However, a subset of samples from both areas plots in the alkali basalt-trachyandesite and trachyte fields. On the Y/Nb vs. Y/Ta petrogenetic plot (Fig. 11b), the samples are spread out in a broad arc, mostly between N-MORB (normal mid-ocean ridge basalt), E-MORB (enriched mid-ocean ridge basalt) and OIB (ocean island basalt). The sample/chondrite plot (Fig. 11c) indicates a wide range of magmatic 'enrichments' from near MORB, through E-MORB, to near OIB. A similar range of 'enrichments' is evident on the sample/MORB vs. selected elements plot (Fig. 11d). All of the tholeiitic volcanics show marked Nb and Ta negative anomalies, whereas the 'enriched' lavas have greatly reduced Nb and Ta negative anomalies. The Th/Yb vs. Ta/Yb plot in Figure 11e compares the present data set with modern Caribbean settings. The Ba/Yb vs. Nb/Yb plot in Figure 11f facilitates comparisons with the modern west Pacific region. The Th/La vs. Sm/La provides indications of the likely sediment contribution to the Yüksekova Complex oceanic arc volcanism. Finally, the La/Nb vs. Y plot (Fig. 11h) compares the data from the eastern Turkish outcrops of the Yüksekova Complex to the larger published data set for volcanics in the Yüksekova Complex, c. 300 km farther west (Kovancılar-Elazığ-Maden area) (see Discussion).

Biostratigraphy of pelagic limestones

Pelagic carbonates associated with the lavas of the Yüksekova Complex (east of Özalp) were previously assigned a Maastrichtian-Palaeocene(?) age based on planktic foraminifera (Şenel et al., 1984; Şenel, 1987). Also, intrapillow pelagic carbonate (N of Lake Erçek) was dated as late Maastrichtian, although these rocks were considered to belong to an Upper Cretaceous ophiolitic melange (Çolakoğlu et al., 2014).

During this study, pelagic limestones were collected from between volcanic rocks in widely spaced outcrops of the Yüksekova Complex throughout the study area (numbered individually in Fig. 2). In thin section, the pelagic limestones (Figs. 8a, 10A-P) are packed with planktic foraminifers in a pink micritic matrix, with minimal clastic material. Previously *Globotruncana (=Contusotruncana) contusa* (Cushman) (late Maastrichtian), *Globotruncana (=Globotruncanita) stuarti* (De Lapparent) and *Globotruncana arca* (Cushman) were reported, indicating a Maastrichtian age, but without locality information (Şenel et al., 1984; Şenel, 1987). During this study, the observed foraminiferal assemblages were found to be consistent with a late Campanian-Maastrichtian age, with one sample (from NW of Özalp, YU24-106) indicating a specifically late Maastrichtian age (Table S1). The age-diagnostic planktic foraminifera include *Globotruncanita stuarti* (Fig. 10A), *Contusotruncana contuse* (Fig. 10B), *Planoglobulina acervulinoides* (Fig. 10C), *Globotruncana falsostuarti* (Fig. 10D) and *Planoglobulina carseyae* (Fig. 10G). The combined biostratigraphical evidence supports a Maastrichtian age, although a partly Campanian age cannot be excluded. A similar age range is reported, also based on planktic foraminifera, in the type area of the Yüksekova Complex farther south (Robertson et al., 2026).

Ophiolitic rocks

No laterally extensive coherent ophiolite is exposed in the study area. However, three small bodies of intrusive ophiolitic rocks have been studied petrographically and geochemically (Günay et al., 2012; Çolakoğlu et al., 2012) (Fig. 2). Two of these, Mehmetalan (Fig. 12a) and Mollatopuz (Fig. 12b) are in the east, and the third Alabayır (Fig. 12c) is near Van city. The ophiolitic fragments are in tectonic contact with Palaeocene to Plio-Quaternary sediments. The Mehmetalan ophiolite fragment (c. 500–600 m thick) is mainly ultramafic tectonites with rare mafic cumulates and pegmatitic gabbro (undated). The Mollatopuz ophiolite fragment includes ultramafic and mafic cumulates. The Alabayır ophiolite fragment is composed of serpentinised harzburgite, dunite, mafic cumulates (olivine gabbro, troctolite and layered gabbro), pyroxenite dykes and chromitite (Çolakoğlu et al., 2012). Harzburgite is the dominant rock type (85-90% by volume) within the mantle peridotites (Üner, 2021). Whole-rock major and trace element compositions of the harzburgite, together with the mineral chemistry of chromites (Cr# 68-79), olivines (Fo92-93) and pyroxenes (Mg#92-94) suggest that the mantle peridotites resulted from the interaction between boninitic melt and peridotite, in a proposed forearc setting (Üner, 2021).

The ultramafic and mafic intrusives are cut by swarms of isolated plagioclase-phyric diabase dykes that vary in thickness from a few metres to tens of metres, and are extensively rhodingitised (Günay et al., 2012; Üner, 2021). The dykes in the Mehmetalan and Mollatopuz ophiolite fragments trend c. east-west, whereas in the Alabayır ophiolite fragment they trend c. NE-SW.

Chemical analysis of the diabase dykes from the Mehmetalan and Mollatopuz ophiolites shows that they range from compositions typical of N-MORB, to enriched MORB (E-MORB), and mostly exhibit negative Nb-anomalies, pointing to a supra-subduction zone origin. In contrast, the dykes of the Alabayır ophiolite are similar to ocean island basalt (OIB). Decompression melting induced by slab rollback during the Late Cretaceous closure of the southern branch of the Neotethys is inferred to have played a key role in the generation of both the depleted and the enriched magmas (Çolakoğlu et al., 2012) (see Discussion).

A Ti-augite-phyric diabase dyke (E-MORB) cutting the Mollatopuz ophiolite fragment has yielded an Ar/Ar plateau age of 105.4±1.1 Ma (Albian), whereas a SSZ-type dyke from the Mehmetalan ophiolite fragment has been dated as 92.0±0.9 Ma (Turonian). A dyke from the Alabayır ophiolite fragment gave a preliminary Ar/Ar whole rock plateau age of 87.7±1.0 Ma (late Coniacian) (Günay, 2011). Thus the dyke intrusion apparently extended over c. 17 Ma and does not overlap with the palaeontologically determined age of the Yüksekova Complex volcanics (see Discussion).

Ophiolite-related melange

The ophiolite-related melange (Bakışık Melange and Olistostrome of Sümengen, 2008a,b,c) includes a wide variety of both ophiolitic and non-ophiolitic rocks and is reported to underlie the ophiolitic fragments (e.g., Mehmetalan ophiolite) (Sümengen, 2008a,b,c). Because a sedimentary (i.e., ‘olistostromal’) origin has not yet been convincingly demonstrated, we prefer to term this unit simply as the Bakışık Melange. The ophiolitic rocks (see above) and the heterogeneous ophiolite-related melange were not mapped separately by MTA. However, good examples of the ophiolite-relate melange occur east Lake Erçek and north of Van, where the melange is soft weathering and has a low relief (Fig. 6h). The following lithologies are recorded as blocks within the ophiolite-related melange: ophiolitic rocks including serpentinised harzburgite, dunite, gabbro and basic volcanics; deep-sea sedimentary rocks, mainly radiolarian chert, pelagic limestone and mudrock (shale), and probably also neritic sedimentary rocks (marble, dolomite). In different exposures, the matrix ranges from sheared serpentinite to sheared clastic sedimentary rocks (e.g., siltstone, sandstone, conglomerate). Most of the lithologies have undergone only low-grade metamorphism but metabasic rocks are reported locally (Sümengen, 2008a,b,c). Detailed research remains to be carried out on the melange; e.g. to determine tectonic versus sedimentary origins.

Paleozoic-Mesozoic unit

The study area east of Lake Van is characterised by generally east-west trending, discontinuous outcrops of low-grade metamorphic rocks, of mainly metasedimentary origin. The exposures range from semi-continuous over >10 km laterally, to isolated blocks (Fig. 2). No complete Palaeozoic-Mesozoic succession is exposed within the study area. Mapping by MTA (Şenel et al., 1984; Şenel, 1987; Sümengen, 2008a,b,c) revealed partial successions, separated by unconformities and structural breaks, as shown in Figure 14b. The unit extends northwards beyond the study area until it is covered by younger sediments and volcanics. Close to the Iranian border (east of the study area a relatively complete virtually unmetamorphosed succession (Hasandağı Unit) is reported to be made up of Palaeozoic dominantly terrigenous clastic sediments and Jurassic-Cretaceous mainly neritic carbonates (Şenel et al., 1984; Şenel, 1987) (see also Fig. 4).

The stratigraphically lowest levels of the Palaeozoic succession (Tepedam Metamorphics; up to c. 700m thick) are locally exposed in the east (east of Özalp) (Figs. 2, 14b), where they are made up of alternating low-grade metamorphosed terrigenous sandstone, siltstone, mudrock (shale), dolomitic limestone and calcareous mudrock (marl), and include a shallow-water limestone interval (Marble Member; c. 150m thick). Meta-volcanics (metabasite, chlorite-schist, metatuff) occur in the upper levels of this succession. After a break (possible unconformity), the succession is dominated by clastic sediments (Yamanyurt Formation; up to 700m thick). Quartzose sandstones, siltstones, minor pebbly conglomerates and dolomitic shallow-water limestones (c. 50m thick), together with andesites (Yüksektepe Formation, c. 700m), are reported locally near Özalp (SE of Emek). In a small area in the northeast, medium-thick bedded limestones, locally dolomitic (Ziyarettepe Formation) include poorly preserved tabulate and rugose corals (Disphyllids and Zaphrentids), suggesting a Mid-Late Devonian age (Şenel et al., 1984; Şenel, 1987). Elsewhere in the east (east of Özalp), dark-coloured shallow-water limestones include poorly preserved dasycladalean algae (e.g., *Mizzia* sp.) (Kurbağapınarı Formation), indicating a Late Permian age. North of the study area, a small, isolated NE-SW trending, fault-bounded outcrop of neritic limestone near the northeast shore of Lake Van (near Çolpan), previously mapped as Triassic (MTA, 2011), was recently found to contain small benthic foraminifera and rare fusulinids indicating a Middle Permian age (Capitanian age; Guadalupian epoch) (Atakul-Özdemir, 2019). The fauna correspond to the Southern Biofacies Belt, which is typical of the Tauride crustal units that restore to the northern margin of Gondwana prior to Neotethyan rifting (Altıner et al., 2000). Elsewhere, the

overall succession, as widely exposed north of Lake Erçek, continues with shallow-water limestones and dolomitic limestones (Saltedağı Formation, c. 200m thick; Fig. 6). The benthic foraminifer *Aulotortus* sp. is consistent with a Mid-Late Triassic age (Acarlar et al., 1991). During this study, the mapped Triassic section was found to include greenish altered felsic metavolcanics (Fig. 6j), with a rhyo-dacitic composition (Table S2). Chondrite-normalized rare earth element (REE) and N-MORB-normalized spider plots suggest an enriched source (La/Yb= 12) for the volcanic rock (Table S2). Further chemical analysis remains to be carried out on these rocks.

After a structural break, there is a then thick succession dominated by shallow-water carbonates (Tozutepe Formation; up to 1500m thick), which in places is mapped as structurally overlying ophiolite-related melange (Sümengen, 2008a,b,c) (Fig. 14b). This succession begins with sandstone-limestone alternations, with pinkish red micritic and siliceous interbeds, and passes upwards into medium-thick bedded limestones and dolomitic limestones rich in calcareous algae (Balkaş et al., 1980). The benthic foraminifera *Involutina liassica, Opthalmidium* sp., *Trocholina* sp., Textulariidae, *Valvulina* sp. and *Pseudocyclammina* sp., together with the large bivalve *Megalodon* sp., are consistent with a Middle Triassic to Jurassic-Cretaceous age range. Near the Iranian border, the Jurassic-Cretaceous shallow-water carbonates are mapped as overlying the Palaeozoic unconformably or with a sheared (thrust?) contact in different places (Şenel et al., 1984; Şenel, 1987).

The youngest part of the succession (Çomaklı Formation; up to 350m thick) consists of alternations of medium-thick bedded grey to black limestones, together with dolomitic limestone, siliceous limestone, sandstone, conglomerate, pelagic limestone and, notably, volcanic rocks. Benthic foraminifera such as *Pseudocyclammina* sp., *Neotrocholina* sp., *Cuneolina* sp., *Orbitolina* sp., *Salpingoporella* sp., *Dictyoconus* sp. and *Textularia* sp. indicate a Barremian–Cenomanian age (Sümengen, 2008a,b,c). Intermediate to felsic-composition intrusive rocks (diorite, quartz diorite, granodiorite, monzodiorite) (Bazıdağ Magmatics) have been reported from the Palaeozoic-Mesozoic succession near the Iranian border (Şenel et al., 1984; Şenel, 1987). However, these rocks were more recently mapped as intrusive into Upper Cretaceous 'ophiolitic melange' suggesting a different origin (Şenel and Ercan, 2002), potentially related to the Upper Cretaceous Yüksekova Complex.

Upper Palaeocene-Middle Eocene succession

Exposures of Palaeocene-Eocene age are scattered throughout the area east of Lake Van but are most extensive directly northeast of Van city (Figs. 2, 15). There are two different successions, of which the first is exclusively shallow-water carbonates, whereas the second is deeper water, mixed carbonates and siliciclastics. The shallow-water carbonates (Toprakkale Formation) are up to several hundred m thick in the study area (Fig. 15.1), although they are reported to be much thicker elsewhere (Acarlar et al., 1991). In different places, the contact with underlying units is unconformable or tectonic (Sümengen, 2008a,b,c). Mapping in the east, near the Iranian border (east of Özalp), did not reveal any obvious structural break between the Upper Cretaceous Yüksekova Complex and the Palaeocene-Eocene successions, which were described as a single unit (Şehittepe Formation) (Şenel et al.,1984; Şenel, 1987). Farther west (present study area), the base of the Palaeocene-Eocene succession (Toprakkale Formation; Fig. 15.1) is commonly covered by talus (Fig. 16b) but where observable the basal contact is generally sheared and brecciated (e.g., NE of Van city; Fig. 16c), although a normal contact is likely in places (e.g., north of Akgöl; Fig. 2).

The basal levels of the succession (< 5m thick) commonly include a mixture of quartz and micritic carbonate grains in a silty matrix (Fig. 8c). The lithoclasts (e.g., monocrystalline quartz and volcanic rock fragments) are consistent with derivation from the Upper Cretaceous Yüksekova Complex. A basal breccia-conglomerate (derived from the Yüksekova Complex) locally includes rounded clasts of shallow-water limestone, indicative of syn-depositional reworking (Fig 16a; see also Discussion).

Higher levels of the Upper Palaeocene-Middle Eocene succession (Yücelendere Formation; Fig. 15.2) contain abundant calcareous algae and benthic foraminifera, largely reworked (Figs. 8d-i; 17a,b). Of the previously reported benthic foraminifera (Şenel et al.,1984; Şenel, 1987; Acarlar et al., 1991; Sümengen, 2008a,b,c), *Miscellanea* cf. *miscella*, *Anatoliella ozalpiensis* and *Dictyokathina vanica* are specifically Palaeocene, whereas *Miscellanea* sp., *Dictyokathina* sp., *Eponides* sp., *Discocyclina* sp. and *Alveolina* sp. are consistent with a generally Palaeocene–Eocene age range.

In the east, near the Iranian border, the Palaeocene is reported to include 'reef limestones' (c. 150 m thick; not illustrated here), with the benthic foraminifera *Broeckinella arabica*, *Glomalveolina primaeva*, *Miscellanea miscella*, *Distichoplax biserialis*, *Alveolina* cf. *pasticillata*m, and the molluscs *Ostrea* cf. *sakaryensis*, *Batillaria subacuta* and *Pseudomiltha* sp. (Şenel et al., 1984; Şenel, 1987).

During this study, samples from several outcrops (numbered in Fig. 2) were dated, mainly using benthic foraminifera and calcareous algae (see Table S2), yielding Palaeocene, Palaeocene(?)-Eocene and Palaeocene-Eocene(?) ages (see Fig. 10 E-P). One sample was specifically dated as Late Palaeocene (YU24-119).

The deeper-water mixed carbonate-siliciclastic succession (Yücelendere Formation, up to c. 250m thick) is mainly exposed in separate areas compared to the Toprakkale Formation (Fig. 15.2); however, a conformable contact is reported in the east (Şenel et al., 1984; Senel, 1987). Marginal facies include lenticular pebbly conglomerate with reworked large foraminifera. Higher levels of the succession are dominated by pinkish pelagic limestone, hemi-pelagic marl, siltstone and sandstone (Fig. 17c). The previously reported planktic foraminifera *Globorotalia* sp., *Globigerina* sp., *Morozovella/Morozovelloides*, sp., *Globigerina* sp., *Globigerinidae, Rotaliidae* and *Textulariidae,* together with the benthic foraminifer *Discocyclina sp.* and *Anomalina* sp., indicate an Eocene age (Şenel et al., 1984; Senel, 1987; Acarlar et al., 1991).

During this study, Eocene was confirmed (Fig. 18A-E) and one sample was dated as specifically Lutetian (YU25-105).

Oligocene-Lower Miocene succession

The mainly siliciclastic Oligocene-Miocene succession (Van Formation=Mendikdere Formation east of Özalp; Şenel et al.,1984; Senel, 1987) is up to 1200m thick, and is equivalent to the regional Kırkgeçit Formation (Perinçek and Özkaya, 1981) (Fig. 15.4). The formation has an unconformable or tectonic contact with the underlying units in different areas (Figs. 3,4).

In some areas, the lower part the succession encompasses patch reefs (Adilcevaz Limestone, up to 500m thick) (Figs. 15.3;16g) that contain diverse corals including *Phyllocoenia lucassiana, Hydronophyllia oligocenia, Cereiophyllia* cf. *tenuis, Heliastraea canals, Astrocoenia bodellei, Tarbellastraea conoidea, T. aquitenestraca*, *Porites collegiana, Astrocoenia ramosa, Heliastraea nerthensis, Cladocora* cf. *manipulate, Goniopora* cf. *globosa, Paleoplesiastraea* cf. *corrugata, Flabellum extensum* and *Balanophyllia* cf. *irregularis* Seguenza. Associated benthic foraminifera include *Lepidocyclina* cf. *tournoueri, Miogypsina* cf. *intermedia, M. irregularis* and *Miogypsinoides* cf. *deharti,* together indicating an Oligocene age. The higher part of the succession is characterised by bioclastic limestones with coral, bivalves and gastropods, pointing to an Oligocene-Early Miocene age for the whole formation (Acarlar et al., 1991).

Away from the shallow-water carbonates, an overall fining-upwards terrigenous clastic succession begins with polymictic conglomerates (5-50m thick), intercalated with reddish-brown siltstone and mudrock (Fig. 17d-h). The clasts match the subjacent lithologies, which include marble and schist, typical of the Palaeozoic-Mesozoic unit, reworked algal limestone (Fig.16l) similar to that of the Palaeocene-Eocene succession, and common chert (of several possible origins) (Fig. 16h). The higher levels of the succession are mainly sandstone, siltstone, marl and calcarenite with subordinate matrix-supported pebbly conglomerates and localised intraformational conglomerates (Fig. 16 i,j). The marls contain planktic foraminifera including *Globigerinoides* cf. *trilobus, G. sicanus, Globorotalia obesa, Globoquadrina cf. dehiscens, Catapsydrax dissimilis* indicating an Early Miocene age (Acarlar et al., 1991; Sümengen, 2008a,b,c).

During this study, observations were restricted to near the base of the succession, mainly to help determine contact relations. A spot sample north of Van city (YU24-122) was dated as Oligocene-Miocene, and another sample from SW of Van city (YU24-123) as Miocene (Table S1).

Between Lake Van and Hakkari to the south, Elmas (1994, 1996) and Elmas and Yılmaz (2003) have reported a sequence of andesite, dacite and rhyolite (Gövelek volcanics) of inferred late Lutetian-Late Oligocene age. Basal olistostromes (ophiolite-derived) and clastic rocks together with reef limestones were reported to pass upwards into alternations of sandstone, conglomerate, mudstone, marl, sandy limestone and pelagic limestone, with local red claystone and gypsum. Analyses of these volcanics indicated a subduction influence. Problems with the identification of these volcanic rocks in the field are considered below. In addition, the above authors advocated four phases of regional deformation and nappe emplacement: Middle Eocene, Late Eocene, Late Oligocene and Early Miocene.

DISCUSSION

Volcanic vs. intrusive Upper Cretaceous units

There are two interpretations of the relationship of the volcanic rocks to the intrusive ophiolitic rocks. The first is that the intrusive ophiolitic rocks represent a discrete tectonic unit, termed the Mehmetalan Peridotite by Şenel et al. (1984) or the Erekdağı ophiolite by Acarlar et al. (1991), based on outcrops in westerly and easterly outcrops, respectively; i.e., separate from the volcanic-sedimentary Yüksekova Complex. The second interpretation is that all of the above lithologies represent ophiolitic melange; i.e., with no specific recognition of a Yüksekova volcanic arc unit east of Lake Van (Çolakoğlu et al., 2014). The available information favours the first interpretation (separate units) for several reasons: (1) the dated dykes cutting ophiolitic peridotites (Fig. 12) range in age from c. 105-88Ma (Albian-Coniacian) (Çolakoğlu et al., 2014), compared to c. 68 Ma (late Maastrichtian) for the lavas that were previously dated using microfossils (Çolakoğlu et al., 2014); (2) Alkaline lavas that co-exist with tholeiitic lavas (Özdemir, 2016; this study) are similar in age (Campanian-Maastrichtian) elsewhere east of Late Van (Gövelek area; this study); (3) Tholeiitic and alkaline lavas are stratigraphically intercalated in the more intact type area of the Yüksekova Complex, near Yüksekova (Robertson et al., 2026). The intrusive ophiolitic rocks and the Yüksekova volcanic-sedimentary rocks are therefore interpreted separately below.

Setting of Upper Cretaceous ophiolitic units

Within the study area, the ophiolitic rocks are mainly represented by depleted mantle harzburgite, dunite and mafic cumulates (Mehmetalan ophiolite; Fig. 12a,b). As noted above, the diabase dykes cutting the peridotites have a wide age range, from c. 105 Ma (Albian) for the E-MORB dyke cutting the Mollatopuz ophiolite fragment, to c. 92 Ma for a SSZ-type dyke cutting the Mehmetalan ophiolite fragment, to c. 88 Ma for the OIB-type dyke cutting the Alabayır ophiolite fragment (Günay, 2011). The c. E-W trend of the dykes in two of the fragments (Mollatopuz and Mehmetalan; Fig. 12a,b) could represent the oceanic spreading fabric in this area, although tectonic rotations cannot be excluded.

The E-MORB dykes could not have resulted from fractionation of SSZ-type magma. Despite its SSZ composition, the *c.* 92 Ma dyke could not have fed the exposed volcanics of the Yüksekova Complex in the study area which, as explained above, are significantly younger (Campanian-Maastrichtian) (Table S1). Also, the 88 Ma (Coniacian) OIB dyke is older than the lavas of the Yüksekova Complex as dated by interlava microfossils (this study). Furthermore, the 105 Ma (Albian)-aged E-MORB dykes predate the *c.* 85-84 Ma (Santonian) (Karaoğlan et al., 2012) ophiolitic rocks (e.g., gabbros and lavas) in the Elazığ area farther west (Fig. 1) (e.g., İspendere and Kömürhan ophiolites; Beyarslan and Bingöl, 2010; Parlak et al., 2013; Rızaoğlu et al., 2006), which, in addition, have a contrasting SSZ arc-type composition.

Here, it is proposed that the three peridotites and associated gabbros in the study area represent fragments of oceanic lithosphere that formed related to early-stage subduction, prior to the development of the Yüksekova volcanic arc. The intrusive rocks could, in part, represent remnants of the oceanic basement of this arc, although no primary stratigraphical contacts between these two units are exposed in the study area. In this interpretation, an explanation is required for intrusion of alkaline magmas into the fore-arc, c. 20 Ma earlier than the eruption of the alkaline lavas associated with the Yüksekova Complex (see below).

Development of the Upper Cretaceous Yüksekova arc

The Yüksekova arc volcanics erupted in a deep-marine oceanic setting, interspersed with pelagic carbonate and minor siliceous (radiolarian) sediments. The available microfossil dating indicates a Campanian-Maastrichtian (possibly mainly late Maastrichtian) age for the volcanism (Şenel et al., 1984; Şenel, 1987; Sümengen, 2008a,b,c; this study; Supplementary Table 1). Concerning the published Ar-Ar ages of the dykes cutting the ophiolitic fragments (Çolakoğlu et al., 2012), the Coniacian-Santonian ages for SSZ and alkaline dykes could be acceptable for feeders to the Yüksekova Complex lavas because they are within (or close to) the recorded age range of the volcanics in the westerly outcrops of the Yüksekova Complex (Kovancılar-Elazığ-Maden) ((c. 86 Ma; Santonian; Ural et al., 2015). However, the Albian (c. 105 Ma) E-MORB dyke significantly predates the oldest known Yüksekova volcanic rocks in the western outcrop, and there is no proof that any of the dated diabase dykes cutting the ophiolitic peridotite fed the Yüksekova arc sequence because they are preserved in different tectonic units. If any of the above dykes fed the Yüksekova volcanics (assuming their reported ages are valid), then the Yüksekova Complex volcanism in the study area would have persisted for a longer period than is currently indicated by the available microfossil ages. However, the Lutetian dyke age is problematic because the Yüksekova Complex is regionally sealed by the Upper Palaeocene-Lower Eocene sedimentary cover (see below).

The combined geochemical evidence from the area east of Van (Fig. 11a-h) shows two overall trends. The first trend is from tholeiitic basalt, to andesite, to basaltic andesite, to rhyolite-dacite (calc-alkaline), typical of an oceanic volcanic arc, such as in the modern SW Pacific region (e.g., Ishizuka et al., 2003, 2011). The second trend is alkaline basalt evolving towards trachyandesite and trachyte, which is less usual compared to W Pacific oceanic volcanic arcs (e.g., Tamura et al., 2009). The type area of the Yüksekova Complex (c. 100 km to the south) shows the same two overall geochemical trends in some similar aged lavas (Maastrichtian) (Fig. 11a-f). This trend is not recorded in the westerly Kovancılar-Elazığ outcrop, however, where the later stage (type 2) lavas are only moderately enriched (E-MORB), as presently known (Fig. 11h). Within the east of Van study area (e.g., around Gövelek; Fig. 2), both the tholeiitic and alkaline lavas occur together within individual stratigraphical sections rather than, for example, representing juxtaposed thrust slices. In the more intact type area of the Yüksekova Complex farther south stratigraphic intercalations of tholeiitic and alkaline lavas (up to >150m thick individually) occur throughout the lower and mid parts of the overall succession, and may extend above this (Robertson et al., 2026). For the type area, six settings have recently been considered to explain the intercalations of tholeiitic and alkaline lavas: (1) mantle heterogeneity; (2) influence of a mantle plume (upper plate; independent of subduction); (3) mantle plume subduction (lower plate); (4) arc-related rifting; (5) slab-tear or disruption; (6) slab break-off. An additional consideration for the present study area is the c. 105 Ma (Albian) E-MORB dyke cutting peridotite (Çolakoğlu et al., 2012), could be explained by a plume influence (Çolakoğlu et al., 2014). However, the c. 30 Ma time difference between the dyke intrusion and the lava eruption questions the applicability of a plume-related mechanism.

In the westerly Kovancılar-Elazığ outcrop, calc-alkaline lavas are dated as largely Santonian-early Campanian using planktic foraminifera (Ural et al., 2014; Ural and Aktaş, 2023) and as late Cenomanian-early Turonian using Radiolaria (Tekin et al., 2015). The tholeiitic lavas are generally dated as Santonian-early Campanian (Ural et al., 2014, 2022) and as late Campanian–late Maastrichtian in different areas, using planktic foraminifera (Ural and Sarı, 2019). Some lavas are also dated as late Cenomanian-early Turonian using Radiolaria (Tekin et al., 2015). Minor basic to felsic intrusions in the westerly outcrops are dated as 80–88 Ma (Cenomanian-Campanian) by zircon U-Pb laser ablation-inductively coupled plasma-mass spectrometry (LA-ICP-MS) (Ural et al., 2021). Overall, the older lavas (type I) (late Cenomanian-early Turonian) have been interpreted as the products of an immature oceanic arc, whereas the more evolved lavas (type II) were considered to have erupted in a rifted back arc setting (Ural et al., 2015).

Taking account of all the outcrops of the Yüksekova arc (present study area; type area near Yüksekova and the westerly outcrops-Kovancılar-Elazığ-Maden), the relatively young Campanian-Maastrichtian-aged volcanics in the area east of Van are likely to represent a relatively late-stage part of the regional-scale volcanic arc system. In view of the deformed and variable outcrops in the study area it is impossible to be specific, but a proximal back-arc segment is suggested for the more coherent type Yüksekova area farther south (Robertson et al., 2026). The lavas and interbedded pelagic limestones that characterise the lower part of the arc-related succession east of Lake Van are similar to those in the lower part of the arc succession in the type area, whereas the upper part of the type area succession is dominated by volcaniclastic mudrocks, sandstones, marls and tuff. Either such sediments did not accumulate in the study area or the upper part of the arc is not exposed; e.g. because of erosion prior to the Late Palaeocene.

Although supporting isotopic data are not available for the Van area, the Th/La vs. Sm/La proxy for subduction input to the magmatic rocks (Fig. 11g) points to sediment involvement in subduction, possibly varying from pelagic to terrigenous. Terrigenous sediment input would be consistent with formation in a relatively narrow basin bordered by rifted continental margins (see below).

Several lines of evidence suggest that the Upper Cretaceous ophiolitic fragments in the Van area (e.g., Mehmetalan ophiolite) are likely to represent forearc oceanic lithosphere: (1) the remnants are little more than pods within sheared ophiolitic melange, which is consistent with intense deformation above a subduction zone; (2) the ophiolite fragments and ophiolitic melange are stated to be structurally underlain by the ophiolite-related melange (Bakışık Melange; Sümengen, 2008a,b,c). This melange is interpreted as a subduction complex that includes ophiolitic rocks, basic volcanics and deep-sea sediments (e.g., radiolarian chert; pelagic limestone); (3) ophiolitic fragments (basalt, gabbro, harzburgite) of similar age (Albian-Cenomanian) occur beneath the Yüksekova Complex in its type area (Robertson et al., 2026).

Eocene-Oligocene volcanism(?)

To the west and southwest of the study area, the widespread Middle Eocene Maden Complex comprises basic to felsic volcanics, which range from subduction-influenced to alkaline (Aktaş and Robertson, 1984; Perinçek and Kozlu, 1984; Yiğitbaş and Yılmaz, 1996; Ertürk et al., 2018). Previously, Elmas (1994, 1996) and Elmas and Yılmaz (2003) reported correlatives of these Eocene volcanics (Gövelek volcanics), interbedded with Eocene-Oligocene mixed carbonate-siliciclastic sediments in a large area extending from Lake Van to Hakkari, c. 100 km to the south. The volcanic rock dated as 44 ± 0.3 Ma (Lutetian) from near Gövelek is consistent with the presence of Eocene volcanics in this area (Özdemir, 2016), although its alkaline composition contrasts with the arc-type lavas reported by Elmas and Yılmaz (2003). On the other hand, Ar-Ar plateau ages obtained from single samples of altered lava should be treated with caution because several processes could affect the reliability of the results (Chang et al., 2025). Several lines of evidence are difficult to reconcile with the presence of Eocene-Oligocene lavas in the study area: (1) lavas around Gövelek were dated as Campanian-Maastrichtian during this study (see above) and were previously shown as Upper Cretaceous Yüksekova Complex by Çolakoğlu et al. (2012, 2014); (2) lavas were not observed interbedded with the Cenozoic sedimentary successions during this work; (3) Eocene-Oligocene lavas have not been reported based on mapping much of the area east and southeast of Lake Van (Şenel et al., 1984; Şenel, 1987; Sümengen, 2008a,b,c) or in the Hakkarı (i.e., Yüksekova) area (Robertson et al., 2026 and references); (4) the correlative Helete lavas within the frontal imbricate zone c. 300 km farther west have since been shown to be intruded by Upper Cretaceous granitoids, with Eocene nummulitic limestones forming a transgressive cover (Nurlu et al., 2016). More research is, therefore, needed to test the occurrence of Eocene-Oligocene lavas east of Lake Van and farther south.

Setting of Palaeozoic-Mesozoic continental unit

The recorded geology of the area east of Lake Van began in the Palaeozoic. Previously, the Palaeozoic low-grade metamorphic rocks (Palaeozoic-Mesozoic unit) were correlated with both the Bitlis-Pütürge crustal unit and the Malatya-Keban (Tauride) platform, which were interpreted as different parts of a single regional-scale allochthon (Sümengen, 2008a,b,c). However, in most recent interpretations these two units have been interpreted as different crustal blocks, separated by the Berit Ocean (or equivalents) (e.g., Robertson et al., 2006; Barrier et al., 2018; Ural et al., 2021). Prior to the Mesozoic formation of this Neotethyan ocean basin, both the Malatya-Keban and the Bitlis-Pütürge crustal units formed part of the northern continental margin of Gondwana (e.g., Göncüoğlu and Kozlu, 2000) and could thus have similar stratigraphic successions for this early time interval.

The succession in the Malatya-Keban crustal block to the west of the study area is mainly Permian-Late Cretaceous (Perinçek and Kozlu, 1984) but in the west begins in the Late Devonian (?)-Carboniferous (Robertson et al., 2021 and references). Middle-Upper Devonian corals (e.g., *Disphyllum* sp. and *Zaphrentis* sp.) in the Palaeozoic-Mesozoic unit in the study area (Ziyarettepe Formation; Şenel et al., 1984, Şenel, 1987) are similar to well dated Upper Devonian corals in the Bitlis crustal unit (Göncüoğlu and Turhan, 1984; Denayer and Hoşgör, 2021). The underlying terrigenous clastics (Tepedam Metamorphics) of the Palaeozoic-Mesozoic unit, interpreted as Early Palaeozoic in age, are similar to terrigenous clastics in the Bitlis crustal unit (Şenel et al., 1984, 1987; Sümengen, 2008a,bc; Fig. 14a). The Permian is characterised by shallow-water shelf carbonates, as confirmed by the Middle Permian (Tauride) facies exposed near the northeast coast of Late Van (Atakul-Özdemir, 2019). The Triassic records rifting, subsidence and localised alkaline volcanism, followed by Jurassic-Cretaceous development of a subsiding shallow-water carbonate platform. A similar development is known for both the Malatya-Keban platform (Kaya and Bozkaya, 2024) and the Bitlis and Pütürge crustal units (Göncüoğlu and Turhan, 1984; Fig. 14a). As a possible distinguishing feature between these two regional units, however, the Cretaceous volcanic rocks reported from the Palaeozoic-Mesozoic unit (Çomaklı Formation; Sümengen, 2008a,b,c) have potential counterparts in the Malatya-Keban platform (Robertson et al., 2007; Rızaoğlu et al., 2009; Karaoğlan et al., 2016) but volcanics of this age are unknown in the Bitlis and Pütürge crustal units. Despite this, large arc-type intrusions (Baskil Magmatics) are not reported from the Palaeozoic-Mesozoic unit, and more research is needed on the age and geochemical affinities of the Çomaklı Formation (or equivalents).

Two options are: (1) the Palaeozoic-Mesozoic unit correlates with the Tauride Malatya-Keban platform farther west (MTA, 2011; Atakul-Özdemir, 2019) (Fig. 20a,b1). In this case, the Palaeozoic-Mesozoic succession was detached from its inferred crustal basement and was thrust southwards over the other units of the suture zone probably during the Late Eocene (see below); (2) the Palaeozoic-Mesozoic unit correlates with the Bitlis crustal unit to the south (Fig. 20bii). This option implies that the Bitlis continental crust extended far to the north of its present exposure, followed by detachment down to an Early Palaeozoic stratigraphic level and then by southward overthrusting (>100 km) to reach its present most southerly extent.

Consistent with the first option, the outcrop east of Lake Van extends southwards into the Mordağ metamorphic unit [Mordağ Metamorphics of Perinek, 1990; also known as the Mordağ metaophiolite (Elmas and Yılmaz, 2003) and as Upper Cretaceous metamelange (MTA, 2011)]. The Mordağ metamorphic unit is dominated by metamorphosed ophiolite-related rocks (e.g., metalava, metagabbro, serpentinite, amphibolite) (Perinçek, 1990), together with some meta-terrigenous rocks (e.g., schist, quartzite, phyllite), recrystallised carbonates (marble), and associated deep-sea sedimentary rocks (radiolarite, pelagic limestone). The Mordağ Metamorphics have been correlated with the Kömürhan metaophiolite east of Malatya and the Berit metaophiolite in the Elbistan area (Perinçek and Kozlu, 1984). The Mordağ metamorphic unit structurally overlies the Yüksekova Complex in its type area farther south and passes westwards into the Bitlis crustal unit (Perinçek, 1990; Şenel and Ercan, 2002; Fig. 14a). According to Elmas and Yılmaz (2003), the Bitlis crustal unit (Bitlis Metamorphics) terminates eastwards at a major NE-SW left-lateral fault (Narlı-Özalp Fault). However, there is no outcrop east of Gürpınar (Fig.2) and this fault is not indicated on the 1: 125,000 scale map of Türkiye (MTA, 2011). Also, c. 45 km to the southeast of the delineated fault, east of Hakkari, meta-sedimentary rocks (marbles, calc-schists and pelitic schists), rather than meta-ophiolitic rocks, structurally overlie the Yüksekova Complex (Robertson et al., 2026).

Restoring the tectonostratigraphy

There is no easily recognisable ordered tectono-stratigraphy in the study area east of Lake Van (Fig. 2). All of the major units are mapped as being structurally overlain by different units in one place or another (e.g., Figs. 3, 4). An effective way to interpret the geological development is, however, to the structural events (i.e., from younger to older), taking account of the known ages of units and the major stratigraphical unconformities and erosion events, as summarised below.

The Oligocene-Miocene marine sediments and the older units are unconformably covered by the Upper Miocene-recent (neotectonic) units (e.g., Figs. 3, 4), pointing to a marked change in tectonic regime. In some areas, neotectonic units (e.g., Pliocene) are mapped as being overthrust by older units (e.g., Mehmetalan ophiolite) (Fig. 12b), although the distance of displacement is likely to be minor.

In some areas, the Oligocene-Lower Miocene marine sediments are mapped as unconformable on older units, for example, on the Palaeocene-Eocene southeast of Lake Erçek, and the Upper Cretaceous Yüksekova Complex east of Özalp (e.g., Fig. 4). More commonly, the Oligocene-Lower Miocene sediments are overlain structurally by older units [e.g., Yüksekova Complex, ophiolite/ophiolite-related melange, Palaeozoic-Mesozoic unit (e.g., Figs. 3, 4; 19f)]. Taken together, the evidence indicates a major Late Eocene-Early Oligocene(?) compressional event of folding and thrusting.

East of Van city, the Late Palaeocene-Middle Eocene is mapped as locally overlying the Upper Cretaceous Yüksekova Complex with a normal or a tectonic contact in different places (Figs. 16c, 19b-e). In places in the east (east of Özalp), Palaeocene-Eocene sediments have been mapped as overlying Upper Cretaceous volcanogenic rocks, depositionally (Şehittepe formation). These two units were interpreted as a single stratigraphical succession [Şehittepe formation of Şenel et al. (1984) and Şenel (1987)], although an unconformity between them is likely because the Yüksekova Complex formed in a deep sea whereas the Palaeocene is neritic. Alternatively, the Palaeocene-Eocene is locally mapped as above the Late Oligocene-Early Miocene, in places (Sümengen, 2008c). Overall, the Late Palaeocene-Middle Eocene succession is unconformable on the Yüksekova Complex but the succession was later disrupted and intersliced with other units.

The structural position of the ophiolitic fragments (Fig. 12a-c), relative to other units is difficult to assess because they are in tectonic contact with younger units (Figs. 3, 4, 19a). The Yüksekova Complex is commonly intersliced with intrusive ophiolitic rocks, especially serpentinised harzburgite. For example, southeast of Van city (Erekdağı; Fig. 6i), the Yüksekova Complex is locally cut by at least three anastomosing strands of sheared peridotite, each dominated by serpentinised harzburgite. Elsewhere, the Yüksekova lavas are commonly sheared with instances of crosscutting fabrics related to multiphase thrusting (Fig. 6l). In places, the ophiolite-related melange (Bakışık Melange) appears to be below the ophiolitic melange, as noted above. The ophiolite fragments (e.g., Mehmetalan ophiolite) experienced only low-grade metamorphism, whereas the ophiolite-related melange includes metabasic rocks, consistent with the melange representing the structurally lower of these two units.

In many areas, the Palaeozoic-Mesozoic unit is thrust over the Oligocene-Miocene sediments, the ophiolite-related units, and/or the Yüksekova Complex (Figs. 3, 4). On the other hand, in the east (Quadrangle L52), ophiolite-related melange (Bakışık Melange) is locally mapped as above the Palaeozoic-Mesozoic unit (Şumengen, 2008b). The main constraint on the timing of emplacement of the Palaeozoic-Mesozoic unit is that it was emplaced prior to the Oligocene-Early Miocene, the age of the oldest transgressive unit with abundant metamorphic detritus (e.g., schist, marble) derived from the Palaeozoic-Mesozoic unit.

In summary, the overall regional tectono-stratigraphic order at the time of initial Upper Cretaceous accretion (i.e., excluding cover sediments) is inferred, from the base upwards as: 1) accretionary Bakışık Melange; 2) Mehmetalan ophiolite (fragments); 3) Yüksekova Complex oceanic arc; 4) Palaeozoic-Mesozoic unit (emplaced Malatya-Keban platform) (Fig. 20a). The area studied underwent three major phases of compressional deformation: (1) latest Cretaceous-Early Palaeocene(?); (2) latest Eocene-early Oligocene(?); and (3) Mid-Late Miocene. In contrast, the Late Palaeocene-Late Eocene was extensional. Understanding of the timing of deformation events could, in future, benefit from an improved biochronology.

Regional comparisons

Hints concerning the timing of events also come from regional comparisons. To the southeast, in its type area, the Yüksekova Complex forms a structurally coherent regional-scale allochthon, overthrust by the Mordağ Metamorphics (see above). In its type area, the Yüksekova Complex is structurally underlain by blocks of unmetamorphosed serpentinised peridotite, gabbro (undated) and basaltic volcanics (unpublished data). The volcanics are locally interbedded with radiolarites, dated as Albian-Cenomanian (H. Soycan, pers. com., 2025). The Mordağ Metamorphics are mapped as being unconformably overlain by Oligocene-Miocene sediments in most areas (Quadrangles M51 and N 52-53). These maps show Middle Eocene unconformable on the Mordağ Metamorphics, in places. They also show Palaeocene in the same area but only as isolated outcrops with no mapped contacts with the Mordağ Metamorphics (Quadrangles M52-M52; Şenel and Ercan, 2002; Sümengen, 2008a,b), although this is likely to result from limited exposure. Therefore, the Mordağ Metamorphics were transgressed, at least by the Middle Eocene and probably by the Palaeocene, similar to the area present study area east of Lake Van.

Farther west, in the Kovancılar-Elazığ area (Fig. 1), the large relatively intact Upper Cretaceous ophiolites (i.e., Guleman, İspendere and Kömürhan ophiolites; Rızaoğlu et al., 2006; Parlak et al., 2009, 2013; Bayarslan and Bingol, 2014; Ural et al., 2015) occur at a generally higher structural level than the Upper Cretaceous Yüksekova Complex. In most places, the two assemblages are separated by a thick slice of Middle Eocene volcanics and sediments belonging to the Maden Complex (MTA, 2011). Around Elazığ, the Yüksekova Complex is unconformably overlain by latest Cretaceous sediments (Harami Group) (Yılmaz et al., 1993; Aksoy and Türkmen, 1999; İnceöz, 1999). To the northeast, the Yüksekova Complex is covered by Middle Eocene-Lower Oligocene clastic sediments of the Kırkgeçit Formation (Çelik, 2013), whereas to the south of Elazığ the complex is, in places, unconformably overlain by the Maden Complex (Hempton, 1985). The Maden Complex unconformably overlies the Pütürge Metamorphics in large areas south of Elazığ and south of Malatya (MTA, 2011). In these areas, the Maden Complex is structurally overlain by the regional-scale ophiolites (Guleman, İspendere and Kömürhan), with Upper Palaeozoic-Upper Cretaceous Malatya-Keban crustal unit thrust above (Perinçek and Kozlu, 1984; Yazgan and Chessex, 1991; Yılmaz, 1993; Robertson et al., 1991, 2013). The deformed, low-grade-metamorphosed platform succession in the Keban-Malatya thrust sheet was intruded by Upper Cretaceous magmatic arc-type rocks (Baskil arc) (Parlak, 2006; Rızaoğlu et al., 2006, 2009), and then unconformably overlain by Upper Palaeocene-Middle Eocene shallow-water carbonates (Seske Formation) (Çağlar, 2009), similar to those of the Palaeocene-Eocene succession east of Lake Van. The above brief comparison indicates some differences between the study area east of Lake Van and the Kovancılar-Elazığ area farther west, particularly the absence of large relatively intact ophiolites and the lack of substantial thicknesses of the Middle Eocene Maden Complex in the area east of Lake Van.

Development of the suture zone

The information from east of Lake Van and the comparisons with areas farther south (Yüksekova Complex type area) (Perinçek and Özkaya, 1981; Perinçek, 1978, 1990) and west (Kovancılar-Elazığ-Maden) indicate that all three areas are related to the Berit Suture Zone.

At the end of the Cretaceous, the following tectonic organisation is inferred, from south to north: (1) subduction complex (ophiolite-related melange); (2) forearc-ophiolite (exposed on the seafloor or buried); (3) oceanic volcanic arc; (4) unrecorded gap (of unknown width) (Fig. 20a). The unrecorded gap in the north potentially represents oceanic crust that separated the Yüksekova arc from the Malatya-Keban continental platform (Palaeozoic-Mesozoic unit) but is not now preserved.

After erosion, the Yüksekova arc rocks were transgressed during the Late Palaeocene-Middle Eocene (Toprakkale Formation=regional Seske Formation). It is uncertain if the Palaeozoic-Mesozoic unit was also transgressed during this time in the study area. However, assuming the general correlation with the Mordağ metamorphics to the south (see above), this unit was also transgressed during the Palaeocene-Eocene (MTA, 2002, 2007 a,b).

In the eastern Pontides, the İzmir-Ankara-Erzincan Ocean to the north of the study area is believed to have closed during Selandian-early Thanetian (Mid-Late Palaeocene; *c.* 57–60 Ma) (Kandemir et al., 2019), somewhat earlier than its reported Maastrichtian-Middle Palaeocene (60-70 Ma) closure in the central and western Pontides (Mueller et al., 2019). Farther south, the volcanic-sedimentary Maden Complex rifted during the Early-Middle Eocene (c. 50 Ma) (Yiğitbaş and Yılmaz, 1997; Robertson et al., 2006; Yılmaz, 2019). The overall Upper Palaeocene-Middle Eocene deepening-upwards succession (Toprakkale and Yücelendere Formations; Fig. 15) in the study area could be attributed to regional crustal extension that accompanied rollback of the southern Neotethyan subduction zone (Robertson et al., 2006; Robertson and Parlak, 2025) (Fig. 21a). This explanation is preferred rather than the inference of Middle Eocene compression and nappe emplacement (Elmas, 1996).

By the Late Eocene, collision of the over-riding (Tauride) plate with the Arabian continent had begun (Darin and Umhoefer, 2022; Robertson and Parlak, 2025). This is likely to have triggered the progressive deformation of the over-riding plate, potentially a setting of subduction zone roll-forward, with consequent frontal imbrication, crustal loss, and absence of a substantial South Neotethyan accretionary prism (Late Eocene-Early Miocene). As convergence continued, the over-riding crust including the pre-existing Berit Suture Zone was re-imbricated and thrust southwards, prior to the Oligocene-Early Miocene sedimentary transgression (Fig. 20bi). Final closure of the Southern Neotethys (farther south) and 'hard collision' with Arabia took place during the Early Miocene (Yılmaz, 1993; Yılmaz et al., 2023; Robertson and Parlak, 2025).

During the Oligocene-Early Miocene, the study area formed part of the lower plate of the collision-thickened Eurasian periphery (Yılmaz and Yiğitbaş, 2024). Regional compression resulted in flexural collapse to form a foreland basin, in which deepening-upwards gravity-flow deposits accumulated (Van Formation=Kırkgeçit Formation) (Fig. 21b). During the Early Miocene (c. 19 Ma), sedimentation transitioned from deep marine to continental and shallow marine, culminating in an overfilled foreland basin (e.g., Gülyüz et al., 2020). The initial uplift of the East Anatolian Plateau and the onset of intra-continental volcanism ensued during the Late Miocene (Kayın and İşseven, 2023; Yılmaz et al., 2023). Continuing regional convergence was mainly accommodated by Plio-Quaternary left-lateral strike-slip/transpression and westward tectonic 'escape' (Koçyiğit, 2013; Görür et al., 2015; Özalp et al., 2016; Çukur et al., 2017), accompanied by localised overthrusting in the area east of Lake Van.

In summary, our proposed tectonic model for the present study area east of Lake Van is similar to that for the western outcrop of the Berit Suture Zone (Fig. 22a-c) but with several important differences. In the west, the Berit ocean represents a small Mesozoic oceanic basin between the Bitlis and Pütürge continental units to the south and the Malatya-Keban continental platform to the north. Supra-subduction zone spreading took place within the Berit Ocean to form future ophiolitic crust during the Late Cretaceous (Fig. 22a). With continuing closure, double subduction (northwards) generated the Yüksekova oceanic arc and the continental margin Baskil arc (Fig. 22b). The southern part of the Berit Ocean closed by latest Cretaceous-Early Palaeocene(?); however, whether or not any oceanic crust still remained between the Yüksekova volcanic arc and the Malatya-Keban platform is uncertain because of absence of relevant exposure (Fig. 22c). The main differences between the eastern and western areas, however, are: (1) there is no evidence of an equivalent of the Bitlis continental unit in easternmost Anatolia (although subduction or faulting out cannot be exluded); (2) no large-scale equivalents of the Baskil arc are confirmed in easternmost Anatolia (although the ages of several granitic bodies are uncertain); (3) The inferred equivalents of the Malatya-Keban platform (Palaeozoic-Mesozoic unit and the Mordağ metamorphics) in easternmost Anatolia were thrust relatively much farther south than in the type area of the Berit Suture Zone in the west (i.e., almost reaching the Arabian platform in places). (4) The Berit Suture Zone in easternmost Anatolia experienced more complex and extensive re-imbrication, mainly related to Eocene and younger post-collisional tectonics, compared to its type area farther west; (5) In contrast to farther west, there is no equivalent to the rifted basin with extensive volcanics, as represented by the Middle Eocene Maden Complex.

CONCLUSIONS

1) The study area east of Lake Van is interpreted as an eastward extension of the Berit Suture Zone although with some significant differences including absence of exposed Bitlis continental crust to the south, lack of significant Eocene volcanism, thrust emplacement farther south, and a more complex and variable deformation history.

2) Northward subduction of the Berit Ocean in the study area during the Late Cretaceous generated subduction melange (Bakışık Melange), supra-subduction zone oceanic crust (future fore-arc ophiolite) and a regional-scale oceanic volcanic arc (Yüksekova Complex).

3) A dismembered thrust sheet of Palaeozoic-Mesozoic mainly sedimentary rocks (Palaeozoic-Mesozoic unit) is restored as a Palaeozoic terrigenous succession, overlain by Triassic rift-related alkaline volcanics and sediments, and then by a Jurassic-Cretaceous passively subsiding carbonate platform.

4) The above Palaeozoic-Mesozoic unit is interpreted as a southerly overthrust extension of the Malatya-Keban platform farther west, which together represent the northern rifted margin of the Mesozoic Berit Ocean.

5) Following erosion, the Berit Suture Zone was transgressed by shallow-marine carbonates and deeper marine terrigenous sediments during Late Palaeocene-Middle Eocene, in an inferred extensional setting, potentially related to rollback of the Southern Neotethyan subduction zone.

6) Mid-Late Eocene initial closure of the Southern Neotethys and eventual Early Miocene 'hard' collision with the Arabian continent triggered rethrusting and tectonic mixing of the

Berit suture zone in the study area east of Lake Van, including final southward overthrusting and re-imbrication of the dismembered Palaeozoic-Mesozoic platform unit.
7) This key part of the Berit Suture Zone has been disentangled by backstripping, in particular, the timing of deformation events, depositional units and unconformities. Three main compressional events are inferred (latest Cretaceous-Palaeocene(?), Late Eocene-Early Oligocene(?); Mid-Late Miocene, whereas the Late Palaeocene-Middle Eocene was extensional.
8) The Berit Suture Zone represents a major part of the long-recognised East Anatolian Accretionary Complex. More recent inference that the suture zone is underthrust by (Tauride) continental crust does not exclude continued its interpretation as an accretionary complex because this formed during the latest Cretaceous long prior to collision-related crustal underthrusting.

ACKNOWLEDGEMENTS

We thank Ayhan Zenginoğlu and Özgür Yavaş for preparing the thin sections, and Ertuğrul Çanakçı for geochemical sample preparation. Yağız Demirtay is thanked for assistance with drafting the diagrams.

REFERENCES

Acarlar M., Bilgin A.Z., Erkal T., Güner E., Şen A.M., Umut M., Elibol E., Gedik L., Hakyemez Y. and Oğuz, M.F., 1991. Geology of the east and north of Lake Van. Gen. Dir. Miner. Res. Explor., Report No: 9469 (unpublished), Ankara.

Aksoy E., Türkmen İ., Turan, M. and Meriç, E., 1999. New findings on stratigraphic position and depositional environment of Harami Formation (Upper Campanian-Maastrichtian), South of Elazığ. Bull. Turk. Assoc. Pet. Geol., 11: 1–15.

Aktaş G. and Robertson A.H.F., 1984. The Maden Complex, SE Turkey: evolution of a Neotethyan continental margin. In: J.E. Dixon and A.H.F. Robertson (Eds.), Geological Evolution of the Eastern Mediterranean, Geol. Soc. London Spec. Publ., 17: 375–402 https://doi.org/10.1144/GSL.SP.1984.017.01.27

Altıner D., Özkan-Altıner S., Koçyiğit A., 2000. Late Permian foraminiferal biofacies belts in Turkey: Palaeogeographic and tectonic implications. In: E. Bozkurt, J. A. Winchester and J. D. A. Piper (Eds.), Tectonics and magmatism in Turkey and the surrounding area, Geol. Soc. London Spec. Publ., 173: 83–96. https://doi.org/10.1144/GSL.SP.2000.173.01.04.

Atakul-Özdemir A., 2019. Paleogeographic implications of the Permian shallow marine carbonates in the eastern Lake Van region (eastern Turkey): Foraminiferal biostratigraphic and sequence stratigraphic constraints, Geol. J., 54: 2716-2730. https://doi.org/10.1002/gj.3476

Balkaş O., Serdar S.H., Erakman B., Güngör A., Pasin C., Aksu R. ve Işbilir, M., 1980. Başkale-Gürpınar-Çatak-Van alanının jeolojisi ve petrol olanakları: TPAO AramaGrubu, Rapor No: 1455 (yayımlanmamış), Ankara.

Barrier E., Vrielynck B., Brouillet J.F. and Brunet M.F., 2018. Paleotectonic Reconstruction of the Central Tethyan Realm. Tectonono-Sedimentary-Palinspastic Maps from Late Permian to Pliocene: CCGM/CGMW, Paris, Atlas of 20 maps (scale: 1/15.000.000).

Beyarslan M. and Bingöl A.F., 2000. Petrology of a supra-subduction zone ophiolite (Kömürhan-Elazığ-Turkey): Can. J. Earth Sci., 37: 1411–1424. https://doi.org/10.1139/e00-041

Beyarslan M. and Bingol A.F., 2010. Ultramafics and Mafic Bodies in Cumulates of Ispendere and Kömürhan Ophiolites (SE Anatolian Belt, Turkey). Turk. J. Sci. Technol., 5(1): 19-36.

Beyarslan M. and Bingöl A.F., 2018. Zircon U-Pb age and geochemical constraints on the origin and tectonic implications of Late Cretaceous intra-oceanic arc magmatics in the Southeast Anatolian Orogenic Belt (SE-Turkey): J.Afr. Earth Sci., 147: 477–497. https://doi.org/10.1016/j.jafrearsci.2018.07.001

Bingöl A.F., 1984. Geology of Elazığ area in the Eastern Taurus region. In: O. Tekeli and M.C. Göncüoğlu (Eds.), The geology of the Taurus belt. Int. Symp. Proc., Ankara, Turkey, 209-216.

Bingöl A.F. and Beyarslan M., 2023. New Insıght into a Subductıon-Related Orogen: A Reappraısal of the Geotectonıc Framework and Evolutıon of the Middle and West Parts of the Southeast Anatolıan Orogenıc Belt (Türkiye). Asian J. Geol. Res., 6(2): 119-146. https://www.sdiarticle5.com/review-history/103681

Çağlar M., 2009. Benthic foraminiferal biostratigraphy of the tertiary sediments from the Elazig and Malatya Basins, Eastern Turkey. J. Geol. Soc. India, 74(2): 209-222. https://doi.org/10.1007/s12594-009-0123-8

Çelik H., 2013. The effects of linear coarse-grained slope channel bodies on the orientations of fold developments: A case study from the Middle Eocene-Lower Oligocene Kırkgeçit Formation, Elazığ, eastern Turkey. Turk. J. Earth Sci., 22: 320–338. 10.3906/yer-1202-5

Çetinkaplan M., Pourteau A., Candan O., Koralay O.E., Oberhansli R., Okay A.İ., Chen F., Kozlu H. and Şengün F., 2016. P–T–t evolution of eclogite/blueschist facies metamorphism in Alanya Massif: time and space relations with HP event in Bitlis Massif, Turkey. Int. J. Earth Sci., 105: 247-281. https://doi.org/10.1007/s00531-014-1092-8

Chang, S.C., Shi, W., Wang, Y., Wang, F., 2025. Argon-based geochronology: advances, limitations and perspectives. Natl. Sci. Rev. 12(9), https://doi.org/10.1093/nsr/nwaf277.

Cohen K.M., Harper D.A.T. and Gibbard P.L., 2021. ICS International Chronostratigraphic Chart, 2020/01: International Commission on Stratigraphy, IUGS. www.stratigraphy.org

Çolakoğlu A.R., Günay K., Göncüoğlu, M.C., Oyan V. and Erdoğan K., 2014. Geochemical evaluation of the late Maastrichtian subduction-related volcanism in the southern Neotethys in Van area, and a correlation across the Turkish-Iranian border. Ofioliti, 39: 51-65. doi: 10.4454/ofioliti.v39i2.429

Çolakoğlu A.R., Sayıt K., Günay K. and Göncüoğlu M.C., 2012. Geochemistry of mafic dykes from the Southeast Anatolian ophiolites, Turkey: Implications for an intra-oceanic arc–basin system. Lithos, 132: 113-126. https://doi.org/10.1016/j.lithos.2011.11.023

Çukur D., Krastel S., Tomonaga Y., Schmincke H.U., Sumita M., Meydan A.F., Çağatay M.N., Toker M., Kim S.P., Kong G.S. and Horozal S., 2017. Structural characteristics of the Lake Van Basin, eastern Turkey, from high-resolution seismic reflection profiles and multibeam echosounder data: geologic and tectonic implications. Int. J. Earth Sci., 106(1): 239-253. https://doi.org/10.1007/s00531-016-1312-5

Darin M.H. and Umhoefer P.J., 2022. Diachronous initiation of Arabia–Eurasia collision from eastern Anatolia to the southeastern Zagros Mountains since middle Eocene time. Int. Geol. Rev., 64: 2653–2681. https://doi.org/10.1080/00206814.2022.2048272

Denayer J. and Hoşgör I., 2021. First report of Devonian corals from the Bitlis-Pötürge Massif (SE Turkey): a rare occurrence of corals on the northern margin of Gondwana. Geol. Acta, 19(1): 1-11. https://hdl.handle.net/2268/256380

Dong Y., He D., Sun S., Liu X., Zhou X., Zhang F., Yang Z., Cheng B., Zhao G. and Li J., 2018. Subduction and accretionary tectonics of the East Kunlun orogen, western segment of the Central China Orogenic System. Earth-Sci. Rev., 186: 231-261. https://doi.org/10.1016/j.earscirev.2017.12.006

Elliott T., Plank T., Zindler A., White W. and Bourdon B., 1997. Element transport from subducted slab to volcanic front at the Mariana arc. J. Geophys. Res., 102: 14991–15019. https://doi.org/10.1029/97JB00788

Elmas, A., 1994. An example of the active continental margin volcanism in the Late Lutetian-Late Oligocene interval in Southeast Anatolia: Gövelik Volcanics (Van–Erçek). Turk J. Earth Sci. 3: 43-54.

Elmas, A., 1996. The Late Oligocene nappe emplacement in the Southeast Anatolian Orogenic Belt. Turk J. Earth Sci. 5: 89-98 (in Turkish with an English abstract).

Elmas A. and Yılmaz Y., 2003. Development of an oblique subduction zone—tectonic evolution of the Tethys suture zone in southeast Turkey. Int. Geol. Rev., 45: 827-840. https://doi.org/10.2747/0020-6814.45.9.827

Ertürk M.A., Beyarslan M., Chung S.L. and Lin T.H., 2018. Eocene magmatism (Maden Complex) in the Southeast Anatolian orogenic belt: Magma genesis and tectonic implications. Geosci. Front., 9: 1829-1847. https://doi.org/10.1016/j.gsf.2017.09.008

Floyd P.A., Kelling G., Gökçen S.L. and Gökçen N., 1991. Geochemistry and tectonic environment of basaltic rocks from the Misis ophiolitic mélange, south Turkey. Chem. Geol., 89: 263–280. https://doi.org/10.1016/0009-2541(91)90020-R

Ghazi A.M., Pessagno E.A., Hassanipak A.A., Kariminia S.M., Duncan R.A. and Babaie H.A., 2003. Biostratigraphic zonation and 40Ar–39Ar ages for the Neotethyan Khoy ophiolite of NW Iran. Palaeogeogr. Palaeoclimatol. Palaeoecol., 193: 311-323. https://doi.org/10.1016/S0031-0182(03)00234-7

Göncüoğlu M.C., 2014. Comments on a single versus multi-armed Southern Neotethys in SE Turkey and Iran. IGCP589 Development of the Asian Tethyan realm: Geneses, process and outcome. Abstracts and proceedings, 89–95.

Göncüoğlu M.C., 2019. A Review of the Geology and Geodynamic Evolution of Tectonic Terranes in Turkey. In: F. Pirajno, T. Ünlü, C. Dönmez and B. Şahin (Eds.), Mineral Resources of Turkey. Mod. Approaches Solid Earth Sci., Springer–Cham, 16: 19–72. https://doi.org/10.1007/9

Göncüoğlu M.C., Dirik K. and Kozlu H., 1997. General chracteristics of pre-Alpine terrains in Turkey: Explanatory notes to the terrane map of Turkey. Ann. Géol. Pays Héllen., 37: 515-536.

Göncüoğlu M.C. and Kozlu H., 2000. Early Paleozoic evolution of the NW Gondwanaland: data from southern Turkey and surrounding regions. Gondwana Res., 3(3): 315-324. https://doi.org/10.1016/S1342-937X(05)70290-2

Göncüoğlu M.C. and Turhan N., 1983. Bitlis Metamorfitlerinde yeni yaş bulguları. Bull. Miner. Res. Explor., 95(95-96): 1-5.

Göncüoğlu M.C. and Turhan N., 1984. Geology of the Bitlis metamorphic belt. In: O. Tekeli and and M.C. Göncüoğlu (Eds.), The Geology of the Taurus Belt. Proc. Int. Symp., Ankara, Turkey, 237–244.

Günay K., 2011. Geology, petrology, and chrome ores of Van-Özalp area ophiolites (East-Turkey). Ph.D. thesis, Yüzüncü Yıl University, Institute of Science, 250 pp (Unpublished).

Günay K., Çolakoğlu A.R. and Çakır Ü., 2012. Geochemical properties and rodingitization of diabase dykes cutting peridotites in Yüksekova Complex (Özalp, Van, Turkey). Bull. Miner. Res. Explor., 144: 1–22.

Görür N., Çağatay M., Zabcı C., Sakınç M., Akkök R., Şile H. and Örçen, S., 2015. The late quaternary tectono-stratigraphic evolution of the Lake Van, Turkey. Bull. Miner. Res. Explor., 151(151): 1-46.
Gust D.A., Arculus R.J. and Kersting A.B., 1995. Aspects of magma sources and processes in the Honshu arc. Can. Mineral., 35: 347–365.
Haji S.E., Safari S., Bafti B.S. and Mojallal M., 2020. Saqez–Sardasht goldfield, North Sanandaj–Sirjan Zone, Iran: a tectono-metallogenic analysis. Acta Geol. Sin. (Engl. Ed.), 94: 1693–1710. https://doi.org/10.1111/1755-6724.14586
Hassanipak A.A. and Ghazi A.M., 2000. Petrology, geochemistry and tectonic setting of the Khoy ophiolite, northwest Iran: implications for Tethyan tectonics. J. Asian Earth Sci., 18: 109-121. 10.1016/S1367-9120(99)00023-1
Hastie A.R., Ramsook R., Mitchell S.F., Kerr A.C., Millar I.L. and Mark D.F., 2010. Geochemistry of compositionally distinct late Cretaceous back-arc basin lavas: Implications for the tectonomagmatic evolution of the Caribbean plate. J. Geol., 118(6): 655-676. https://doi.org/10.1086/656353
Hatcher R.D., 2010. The Appalachian orogen: A brief summary. In: R.P. Tollo, M.J. Bartholomew, J.P. Hibbard and P.M. Karabinos (Eds.), From Rodinia to Pangea: The lithotectonic record of the Appalachian region. Bull. Geol. Soc. Amer., 206, 1–19. https://doi.org/10.1130/2010.1206(01)
Hempton M.R., 1985**.** Structure and deformation history of the Bitlis suture near Lake Hazar, southeastern Turkey: Geol. Soc. Amer. Bull., 96(2): 233–243.
Hochstaedter A.G., Gill J.B., Taylor B., Ishizuka O., Yuasa M. and Morita S., 2000. Across-arc geochemical trends in the Izu–Bonin arc: Constraints on source composition and mantle melting. J. Geophys. Res., 105: 495–512. https://doi.org/10.1029/1999JB900125
İnceöz M., 1999. Stratigraphy and depositional environments of Harami Formation (Upper Maastrichtian) in the north of Elazığ. Bull. Assoc. Turk. Pet. Geol., 8: 130–136.
Ishizuka O., Taylor R.N., Yuasa M. and Ohara Y., 2011. Making and breaking an island arc: a new perspective from the Oligocene Kyushu–Palau Arc, Philippine Sea. Geochem. Geophys. Geosyst., 12: Q05005. https://doi.org/10.1029/2010GC003440
Ishizuka O., Uto K. and Yuasa M., 2003. Volcanic history of the back-arc region of the Izu–Bonin (Ogasawara) Arc. In: R.D. Larter and P.H. Leat (Eds.), Intra-oceanic subduction systems: tectonic and magmatic processes. Geol. Soc. London Spec. Publ., 219: 187–205. https://doi.org/10.1144/GSL.SP.2003.219.01.09
Juteau T., 2004. The ophiolites of Khoy (NW Iran): their significance in the Tethyan ophiolite belts of the Middle-East. C. R. Géosci., 336(2): 105-108. DOI: 10.1016/j.crte.2003.12.003
Kandemir Ö., Akbayram K., Çobankaya M., Kanar F., Pehlivan Ş., Tok T., Hakyemez A., Ekmekçi E., Danacı F. and Temiz U., 2019. From arc evolution to arc-continent collision: Late Cretaceous–middle Eocene geology of the Eastern Pontides, northeastern Turkey. Bull. Geol. Soc. Amer., 131(11-12): 1889-1906. https://doi.org/10.1130/B31913.1
Karaoğlan F., Parlak O., Hejl E., Neubauer F. and Kloetzli U., 2016. The temporal evolution of the active margin along the Southeast Anatolian Orogenic Belt (SE Turkey): Evidence from U–Pb, Ar–Ar and fission track chronology. Gondwana Res., 33: 190-208. https://doi.org/10.1016/j.gr.2015.12.011
Karaoğlan F., Parlak O., Klötzli U., Koller F. and Rızaoğlu, T., 2013. Age and duration of intra-oceanic arc volcanism built on a suprasubduction-zone–type oceanic crust in southern Neotethys, SE Anatolia. Geosci. Front., 4: 399–408. https://doi.org/10.1016/j.gsf.2012.11.011

Kaya A. and Bozkaya Ö., 2024. Triassic gypsum layers in Keban Metamorphics, eastern Tauride Belt, Southeastern Turkey: New data about Triassic rifting in northern Tethys margin. Int. Geol. Rev., 66(5): 1046-1066. https://doi.org/10.1080/00206814.2023.2225081

Kayın S. and İşseven T., 2023. New paleomagnetic results from Neogene to Quaternary volcanic rocks of north of the Lake Van, Eastern Turkey. Sci. Rep., 13: 12206. https://doi.org/10.1038/s41598-023-39492-w

Keskin M., 2005. Domal uplift and volcanism in a collision zone without a mantle plume: Evidence from Eastern Anatolia, URL:http://www.mantleplumes.org/Anatolia.html

Koçyiğit A., 2013. New field and seismic data about the intraplate strike-slip deformation in Van region, East Anatolian plateau, E. Turkey. J. Asian Earth Sci., 62: 586-605. 10.1016/j.jseaes.2012.11.008

Koçyiğit A., Yılmaz A., Adamia S. and Kuloshvili S., 2001. Neotectonics of East Anatolian Plateau (Turkey) and Lesser Caucasus: implication for transition from thrusting to strike-slip faulting, Geodin. Acta, 14: 177–195. https://doi.org/10.1080/09853111.2001.11432443

McDonough W.F. and Sun S.S., 1995. The composition of the Proceedings of International Symposium on Geology of the Earth. Chem. Geol., 120(3–4): 223–253.

Moghadam H.S., Corfu F., Stern R.J. and Lotfi Bakhsh A., 2019. The Eastern Khoy metamorphic complex of NW Iran: a Jurassic ophiolite or continuation of the Sanandaj–Sirjan Zone? J. Geol. Soc., 176(3): 517-529. https://doi.org/10.1144/jgs2018-081

MTA, 1987. 1:100,000 Turkish geological map, no : 61 Başkale-K52 sheet. Gen. Dir. Miner. Res. Explor., Ankara.

MTA, 2002.100,000 Hakkari-N52 and N53 Paftası Jeoloji Haritası (Geological Map of the Hakkari- N52 and N53 Quadrangles), Gen. Dir. Miner. Res. Explor., Ankara.

MTA, 2007a. 100,000 Hakkari-M51 Paftası Jeoloji Haritası (Geological Map of the Hakkari-M51 Quadrangle), Gen. Dir. Miner. Res. Explor., Ankara.

MTA, 2007b. 100,000 Hakkari-M52 and M53 Paftası Jeoloji Haritası (Geological Map of the Hakkari-M52 and 53 Quadrangles. Gen. Dir. Miner. Res. Explor., Ankara.

MTA, 2011. Geological map of Turkey 1:250,000. Gen. Dir. Miner. Res. Explor., Ankara.

Mueller M.A., Licht A., Campbell C., Ocakoğlu F., Taylor M.H., Burch L., Ugrai T., Kaya M., Kurtoğlu B., Coster P.M.C. and Métais G., 2019. Collision chronology along the İzmir-Ankara-Erzincan suture zone: Insights from the Sarıcakaya Basin, western Anatolia. Tectonics, 38(10): 3652-3674. https://doi.org/10.1029/2019TC005683

Nurlu N., Parlak O., Robertson A. and von Quadt A., 2016. Implications of Late Cretaceous U–Pb zircon ages of granitic intrusions cutting ophiolitic and volcanogenic rocks for the assembly of the Tauride allochthon in SE Anatolia (Helete area, Kahramanmaraş Region, SE Turkey). Int. J. Earth Sci., 105: 283-314. https://doi.org/10.1007/s00531-015-1211-1

Özalp S., Aydemir B.S., Olgun Ş., Şimşek B., Elmacı H., Evren M., Emre Ö., Aydın M.B., Kurtuluş O., Öcal F. and Can A.Z., 2016. Tectonic deformations in the quaternary deposits of the Lake Van (Edremit Bay), Eastern Anatolia, Turkey. Bull. Miner. Res. Explor., 153(153): 45-61. https://doi.org/10.19111/bmre.58034

Özdemir Y., 2016. Geochemistry of tholeiitic to alkaline lavas from the east of Lake Van (Turkey): Implications for a late Cretaceous mature supra-subduction zone environment. J. Afr. Earth Sci., 120: 7-88. https://doi.org/10.1016/j.jafrearsci.2016.04.018

Parlak O., Höck V., Kozlu H., and Delaloye M., 2004. Oceanic crust generation in an island arc tectonic setting, SE Anatolian orogenic belt (Turkey): Geol. Mag., 141(5): 583-603. https://doi.org/10.1017/S0016756804009458

Parlak O., Karaoğlan F., Rızaoğlu T., Nurlu N., Bağcı U., Höck V., Önal A.Ö., Kürüm S. and Topak Y., 2013. Petrology of the İspendere (Malatya) ophiolite from the Southeast Anatolia: implications for the Late Mesozoic evolution of the southern Neotethyan ocean. In: A.H.F. Robertson, O. Parlak and U.C. Ünlügenç (Eds.), Geological Development of Anatolia and the Easternmost Mediterranean Region. Geol. Soc. London Spec. Publ., 372: 219-24. https://doi.org/10.1144/SP372.11

Pearce J.A., 1982. Trace element characteristics of lavas from destructive plate boundaries. In: R.S. Thorpe (Ed.), Andesites, Wiley, New York, 525–548.

Pearce J.A., 1996. A user's guide to basalt discrimination diagrams. In: Wyman D.A. (ed.) Trace Element Geochemistry of Volcanic Rocks: Applications for Massive Sulphide Exploration. Geol. Assoc. Can., Short Course Notes, 12: 79–113.

Pearce J.A. and Stern R.J., 2006. Origin of back-arc basin magmas: Trace element and isotope perspectives. In: D.M. Christie, C.R. Fisher, S.M. Lee and S. Givens (Eds.), Back-Arc Spreading Systems: Geological, Biological, Chemical, and Physical Interactions. Geophys. Monogr. Ser., 166: 63–86. 10.1029/166GM06

Perinçek D., 1978. V-VI-IX. Bölge (Güneydoğu Anadolu otokton-allokton birimler) jeoloji sembolleri: TPAO Arama Grubu, Arşiv No: 6657 (yayımlanmamış), Ankara.

Perinçek, D., 1990. Stratigraphy of the Hakkari region, Southeastern Anatolia: Bull. Turk. Petrol. Geol. Assoc., 2: 21–68.

Perinçek, D. and Kozlu, H., 1984. Stratigraphical and structural relations of the units in the Afşin-Elbistan-Doğanşehir region (Eastern Taurus). In: O. Tekeli and M.C. Göncüoğlu (Eds.), Geology of the Taurus Belt. Proc. Int. Symp., Ankara, 181-198.

Perinçek, D. and Özkaya, İ., 1981. Tectonic evolution of the northern edge of the Arabian Plate (in Turkish). Yerbilimleri 7: 91–102.

Pessagno E.A., Ghazi A.M., Kariminia M., Duncan R.A. and Hassanipak A.A., 2005. Tectonostratigraphy of the Khoy complex, northwestern Iran. Stratigraphy, 2: 49-63.

Plank T., Kelley K.A., Murray R.W. and Stern L.Q., 2007. Chemical composition of sediments subducting at the Izu–Bonin trench. Geochem. Geophys. Geosyst., 8, Q04I16. https://doi.org/10.1029/2006GC001444

Rizeli M.E. and Wang, K.L., 2023. Multi-stage evolution of the Mehmetalan Ophiolite: Cr-spinel characteristics of podiform chromitites. Int. J. Adv. Nat. Sci. Eng. Res., 7: 61–66.

Rızaoğlu T., Parlak O., Hoeck V. and İşler F., 2006. Nature and significance of Late Cretaceous ophiolitic rocks and their relation to the Baskil granitic intrusions of the Elazığ region, SE Turkey. In: A.H.F. Robertson and D. Mountrakis (Eds.), Tectonic Development of the Eastern Mediterranean region. Geol. Soc. London Spec. Publ., 260: 327-350. https://doi.org/10.1144/GSL.SP.2006.260.01.14

Rızaoğlu T., Parlak O., Höck V., Köller F., Hames W.E. and Billor, Z., 2009. Andean-type active margin formation in the eastern Taurides: Geochemical and geochronogical evidence from the Baskil granitoid (Elazığ, SE Turkey). Tectonophysics, 473(1–2): 188-207. 10.1016/j.tecto.2008.08.011

Robertson A.H.F, 2002. Overview of the genesis and emplacement of Mesozoic ophiolites in the Eastern Mediterranean Tethyan region. Lithos, 65(1-2): 1-67. https://doi.org/10.1016/S0024-4937(02)00160-3

Robertson A.H.F. and Parlak O., 2025. Eocene contractional deformation in the NW corner of the Arabian plate and its relation to Arabia-Eurasia collision in SE Türkiye. Int. Geol. Rev., 67(6): 717-753. https://doi.org/10.1080/00206814.2024.2400696

Robertson A.H.F., Parlak O., Metin Y., Vergili Ö., Taslı K., İnan N. and Soycan, H., 2013. Late Palaeozoic–Cenozoic tectonic development of carbonate platform, margin and oceanic units in the Eastern Taurides, Turkey. In: A.H.F. Robertson, O. Parlak and U.C. Ünlügenç (Eds.), Geological Development of Anatolia and the Easternmost Mediterranean Region. Geol. Soc. London Spec. Publ., 372: 167-218. https://doi.org/10.1144/SP372.16

Robertson A.H.F., Parlak O., Rızaoğlu T., Ünlügenç U.C., İnan N., Taslı K. and Ustaömer, T., 2007**.** Tectonic evolution of the South Tethyan ocean: evidence from the Eastern Taurus Mountains (Elazığ region, SE Turkey), In: A.C. Ries, R.W.H. Butler and R.H. Graham (Eds.), Deformation of Continental Crust: The Legacy of Mike Coward. Geol. Soc. London Spec. Publ., 272: 231-270. https://doi.org/10.1144/GSL.SP.2007.272.01.14

Robertson A.H.F., Parlak O. and Taslı, K., 2026. Upper Cretaceous Yüksekova Complex (type area), easternmost Türkiye: formation and emplacement of a proximal back-arc segment of a Tethyan intra-oceanic arc. Island Arc, 35(1): https://doi.org/10.1111/iar.70054

Robertson A.H.F., Parlak O. and Ustaömer T., 2021. Late Palaeozoic extensional volcanism along the northern margin of Gondwana in southern Turkey: implications for Palaeotethyan development. Int. J. Earth Sci. (Geol Rundsch), 110: 1961–1994. https://doi.org/10.1007/s00531-021-02051-7

Robertson A.H.F., Parlak O., Ustaömer T., Taslı K. and Dumitrica P., 2021. Late Palaeozoic-Neogene sedimentary and tectonic development of the Tauride continent and adjacent Tethyan ocean basins in eastern Turkey: New data and integrated interpretation: J. Asian Earth Sci., 220: 104859, https://doi.org/10.1016/j. jseaes.2021.104859

Robertson A.H.F., Ustaömer T., Parlak O., Ünlügenç U.C., Taslı K. and İnan N., 2006. The Berit transect of the Tauride thrust belt, S. Turkey: Late Cretaceous–Early Cenozoic accretionary/collisional processes related to closure of the southern Neotethys: J. Asian Earth Sci., 27: 108–145. 10.1016/j.jseaes.2005.02.004

Robertson A., Parlak O., Ustaömer T., Taslı K., İnan N., Dumitrica P. and Karaoğlan, F., 2013. Subduction, ophiolite genesis and collision history of Tethys adjacent to the Eurasian continental margin: new evidence from the Eastern Pontides, Turkey. Geodin. Acta, 26(3-4): 230-293. https://doi.org/10.1080/09853111.2013.877240

Saccani E., Allahyari K., Beccaluva L. and Bianchini G., 2013. Geochemistry and petrology of the Kermanshah ophiolites (Iran): Implication for the interaction between passive rifting, oceanic accretion, and OIB-type components in the southern Neo-Tethys Ocean. Gondwana Res., 24: 392–411. https://doi.org/10.1016/j.gr.2012.10.009

Şengör A.M.C., Özeren M.S., Keskin M., Sakınç M., Özbakır A.D. and Kayan, İ., 2008. Eastern Turkish high plateau as a small Turkic-type orogen: Implications for post-collisional crust-forming processes in Turkic-type orogens. Earth-Sci. Rev., 90: 1–48. https://doi.org/10.1016/j.earscirev.2008.05.002

Şenel M., 1987. 1/100.000 ölçekli Açınsama Nitelikli Türkiye Jeoloji Haritaları Serisi, Başkale-H38 (K52) Paftası. Gen. Dir. Miner. Res. Explor., Ankara.

Şenel M., Acarlar M., Çakmakoğlu A., Dağer Z., Erkanol D., Örçen S., Taşkıran M.A., Ulu U., Ünal M.F. and Yıldırım H., 1984. Geology of the area between Özalp (Van)–Iran border (Başkale-K52 (=earlier H38)). Gen. Dir. Miner. Res. Explor., Report No: 7623, Ankara (unpublished).

Şenel M. and Ercan T., 2002. Geological Map of Turkey, 1:500,000, Van sheet. Gen. Dir. Miner. Res. Explor., Ankara.

Sümengen M., 2008a. 1:100,000 Turkish geological map, no: 65 Van-K50 sheet. Gen. Dir. Miner. Res. Explor., Ankara, pp16.

Sümengen M., 2008b. 1:100,000 Turkish geological map, no: 64 Başkale-K51 sheet. Gen. Dir. Miner. Res. Explor., Ankara, pp15.

Sümengen M., 2008c. 1:100,000 Turkish geological map, no: 62 Başkale-L51 sheet. Gen. Dir. Miner. Res. Explor., Ankara, pp24.
Sun S.S. and McDonough W.F., 1989. Chemical and isotopic systematics of oceanic basalts: implications for mantle composition and processes. Geol. Soc. London Spec. Publ., 42: 313–345.
Tamura Y., Gill J., Tollstrup D., Kawabata H., Shukuno H., Chang Q., Miyazaki T., Takahashi T., Hirahara Y., Kodaira S., Ishizuka O., Suzuki T., Kido Y., Fiske R.S. and Tatsumi Y., 2009. Silicic magmas in the Izu–Bonin oceanic arc and implications for crustal evolution. J. Petrol., 50: 685–723. https://doi.org/10.1093/petrology/egp017
Taylor R.N. and Nesbitt R.W., 1998. Isotopic characteristics of subduction fluids in an intra-oceanic setting, Izu–Bonin arc, Japan. Earth Planet. Sci. Lett., 164: 79–98.
Tekin U.K., Ural M., Göncüoğlu M.C., Arslan M. and Kürüm S., 2015**.** Upper Cretaceous Radiolarian ages from an arc–back-arc within the Yüksekova Complex in the southern Neotethys mélange, SE Turkey. C. R. Palevol., 14(2): 73-84. 10.1016/j.crpv.2014.10.002
Topuz, G., Candan, O., Zack, T. and Yılmaz, A., 2017. East Anatolian plateau constructed over a continental basement: No evidence for the East Anatolian accretionary complex. Geology, 45(9): 791-794. https://doi.org/10.1130/G39111.1
Topuz G., Göçmengil G., Rolland Y., Çelik Ö.F., Zack T. and Schmitt A.K., 2013. Jurassic accretionary complex and ophiolite from northeast Turkey: No evidence for the Cimmerian continental ribbon. Geology, 41(2): 255-258. https://doi.org/10.1130/G33577.1
Üner T., 2021. Supra-subduction zone mantle peridotites in the Tethyan Ocean (East Anatolian Accretionary Complex–Eastern Turkey): Petrological evidence for melting and melt-rock interaction. Mineral. Petrol., https://doi.org/10.1007/s00710-021-00760-0.
Ural M. and Sarı M.K., 2019a. Paleogeographic and age findings on planktonic foraminiferal assemblages of Yuksekova Complex in the Northeast of Elazig (Eastern Turkey): IOP Conf. Ser.: Earth Environ. Sci., 362(1): 012146, IOP Publishing. doi 10.1088/1755-1315/362/1/012146
Ural M. and Sarı B., 2019b. New planktonic foraminifera data from the Upper Cretaceous pelagic limestones of the Yuksekova Complex in the Maden Area (Southeast of Elazığ, Eastern Turkey): IOP Conf. Ser.: Earth Environ. Sci., 362(1), 012121, IOP Publishing. DOI 10.1088/1755-1315/362/1/012121
Ural M. and Aktaş M.A., 2023. Quantitative new findings about formation and origin of pillow lavas in the Yüksekova Arc Complex, Elazığ (Eastern Turkey). J. Fac. Eng. Archit. Gazi Univ., 38: 535-545. 10.17341/gazimmfd.985161
Ural M., Arslan M., Göncüoğlu M.C., Tekin U.K. and Kürüm S., 2015. Late Cretaceous arc and back-arc formation within the southern Neotethys: whole rock, trace element and Sr-Nd-Pb isotopic data from basaltic rocks of the Yüksekova Complex (Malatya-Elazığ, SE Turkey). Ofioliti, 40(1): 57-72. doi: https://doi.org/10.4454/ofioliti.v40i1.435
Ural M., Göncüoğlu M.C., Arslan M., Tekin U.K. and Kürüm S., 2014. Petrological and paleontological evidence for generation of an arc-back arc system within the closing southern branch of Neotethys during the Late Cretaceous. Proc. 20th CBGA Congr., Bull. Shk. Gjeol. Spec., 2: 1-54.
Ural M., Sayıt K., Koralay O.E. and Göncüoğlu M.C., 2021. Geochemistry and zircon U-Pb Dates of Felsic-Intermediate Members of the Late Cretaceous Yüksekova Arc Basin: Constraints on the Evolution of the Bitlis–Zagros Branch of Neotethys (Elazığ, E Turkey): Acta Geol. Sin. (Engl. Ed.), 95(4): 1199-1216.
Ural M., Sayıt K. and Tekin U.K., 2022. Whole-rock and Nd-Pb isotope geochemistry and radiolarian ages of the volcanics from the Yüksekova complex (Maden area, Elaziğ, E

Turkey): implications for a late Cretaceous (Santonian- Campanian) back-arc basin in the southern Neotethys. Ofioliti, 47(1): 65-83. doi: 10.4454/ofioliti.v47i1.552

Windley B.F., Alexeiev D., Xiao W., Kröner A. and Badarch G., 2007. Tectonic models for accretion of the Central Asian Orogenic Belt. J. Geol. Soc., 164(1): 31-47. https://doi.org/10.1144/0016-76492006-022

Yazgan E. and Chessex R., 1991. Geology and tectonic evolution of the southeastern Taurides in the region of Malatya. Tr. Assoc. Petrol. Geol., 3: 1–42

Yiğitbaş E. and Yılmaz Y., 1996. New evidence and solution to the Maden complex controversy of the Southeast Anatolian orogenic belt (Turkey). Geol. Rundsch., 85: 250-263.

Yılmaz A., Topuz G., Eken T., Candan O. and Yılmaz H., 2023. Geology of the Eastern Anatolian Plateau (Turkey): a synthesis. Tr. J. Earth Sci., 32: 431-446. 10.55730/1300-0985.1854

Yılmaz Y., 1993. New evidence and model on the evolution of the southeast Anatolian orogeny: Geol. Soc. Amer. Bull., 105(2): 251–271.

Yılmaz Y., 2019. Southeast Anatolian Orogenic Belt revisited (geology and evolution): Can. J. Earth Sci., 56: 1163–1180. https://doi.org/10.1139/cjes-2018-0170

Yılmaz Y., Çemen İ. and Yiğitbaş E., 2023. Tectonics of Eastern Anatolian Plateau; final stages of collisional orogeny in Anatolia. In: E.J. Catlos and İ. Çemen (Eds.), Compressional Tectonics: Plate Convergence to mountain building. Geophys. Monogr. Amer. Geophys. Union, 277: 233–244. https://doi.org/10.1002/9781119773856.ch8.

Yılmaz Y., Yiğitbaş E. and Çemen İ., 2023. Tectonics of the southeast Anatolian Orogenic Belt. In: E.J. Catlos and İ. Çemen (Eds.), Compressional Tectonics: Plate Convergence to Mountain Building. Geophys. Monogr. Amer. Geophys. Union, 277: 203-222. https://doi.org/10.1002/9781119773856.ch8

Yılmaz Y., Yiğitbaş E. and Genç S.C., 1993. Ophiolitic and metamorphic assemblages of southeast Anatolia and their significance in the geological evolution of the orogenic belt**:** Tectonics, 12: 1280-1297.

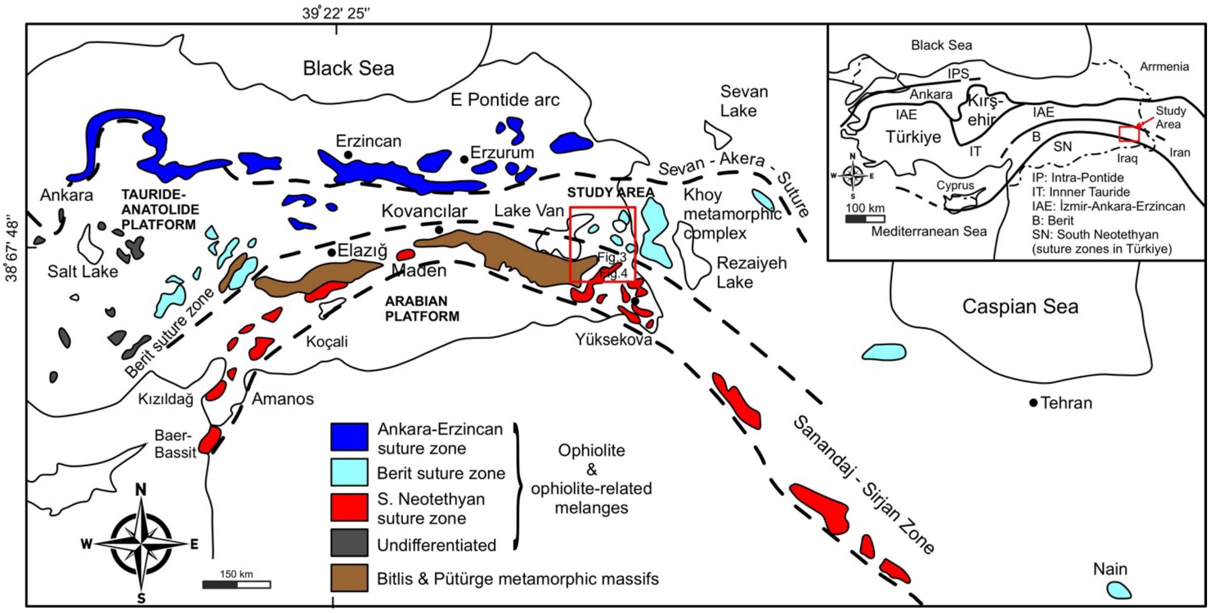

Fig. 1. Outline tectonic map showing the location of the study area east of Van Gölü (Lake Van) (in box; see Fig. 2), and the approximate locations of the more detailed geological maps in Figures 3 and 4. Note the main occurrences of the Upper Cretaceous Yüksekova Complex (red Vs). In SE Turkey, the tectonic units are stacked subvertically over wide areas. The dashed lines indicate the general tectonic trends and not the specific boundaries between major tectonic zones (modified from MTA, 2011 and Göncüoğlu, 2019). Inset: approximate trends of sutures, including the Berit Suture Zone which extends into easternmost Türkiye.

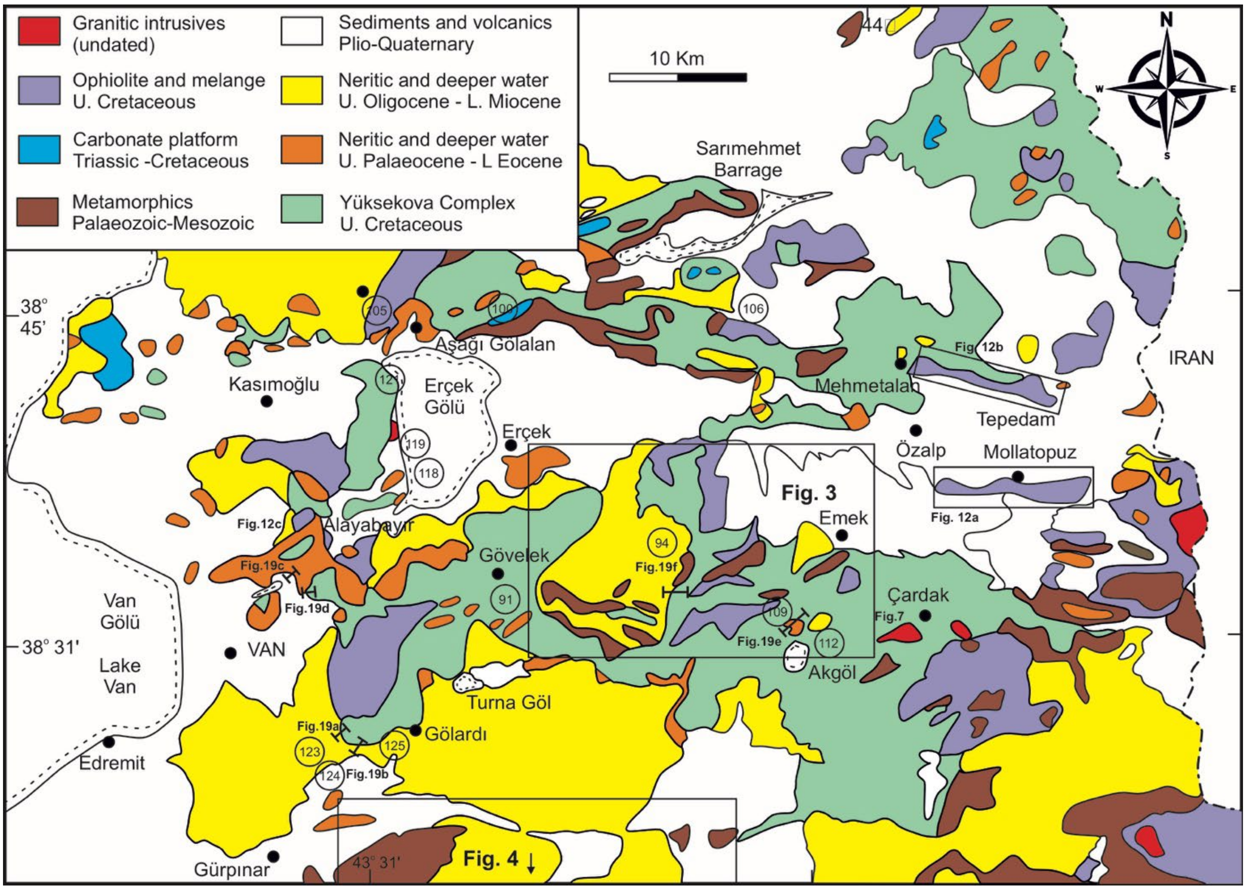

Fig. 2. Outline geological map of the area east of Lake Van. The Upper Cretaceous Yüksekova Complex is widely exposed, whereas ophiolitic rocks mostly occur as relatively small bodies of ordered peridotite-gabbro and more commonly as sheared serpentinite. Miocene-recent volcanics and sediments are not distinguished. See Figs. 3 and 4 for more detailed maps. Figure 4 is located to the south of the area shown here. Simplified from MTA (2011). The locations of samples dated using microfossils are indicated (circles with numbers), as are the locations of copper mineralisation (Fig. 7), three ophiolite fragments (Fig 12 a-c), and structural sections (Fig. 19a-f).

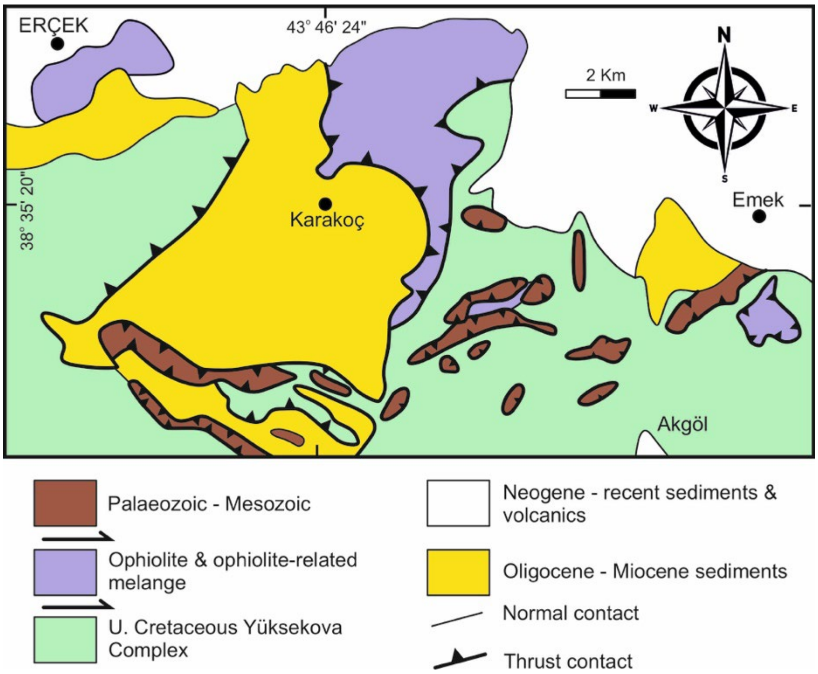

Fig. 3. Example of units exposed within the study area east of Lake Van. Note the complex thrust geometry with the Upper Cretaceous Yüksekova Complex at both low and high structural levels, locally. Simplified from 1:100,000 geological map, Başkale-K51 (Sümengen, 2008a). Sümengen (2008a).

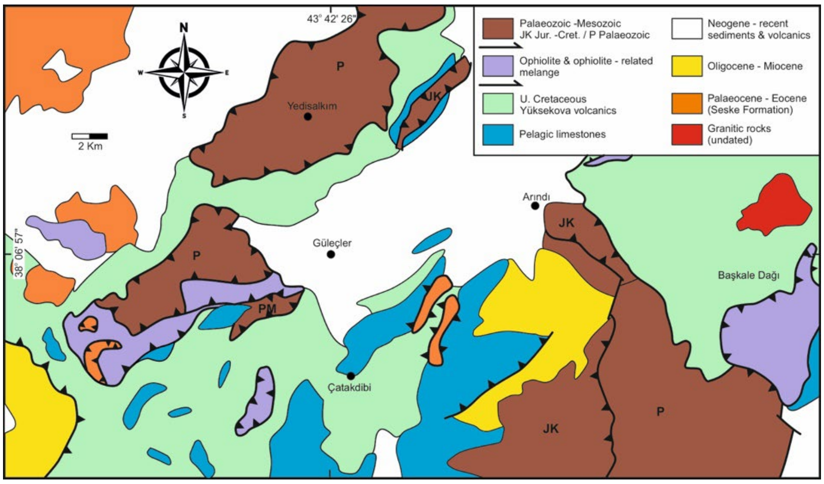

Fig. 4. Example of units exposed in the mountainous region south of the present study area. Simplified from 1:100,000 geological map, Başkale-L51 (Sümengen, 2008c). Note the variable structural geometry with the dismembered Palaeozoic-Mesozoic unit at a relatively high structural level, and the granitic intrusion into the Upper Cretaceous Yüksekova Complex in the east.

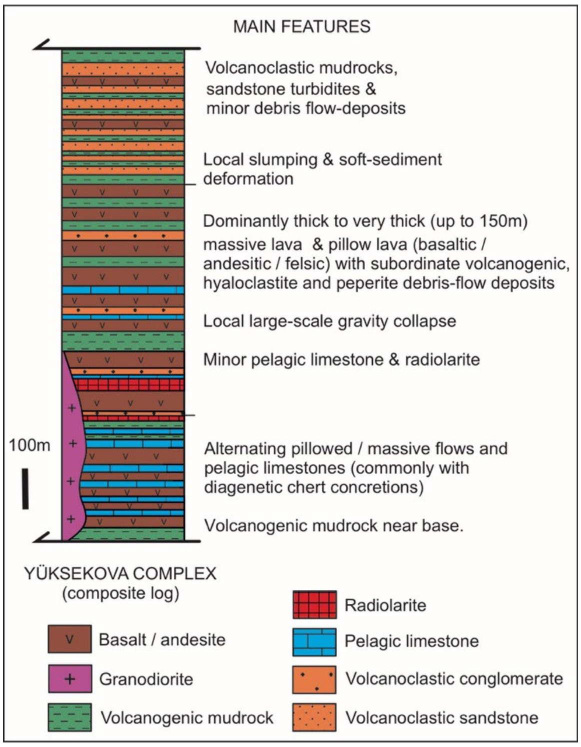

Fig. 5. Generalised stratigraphic log of the Upper Cretaceous Yüksekova Complex in easternmost Türkiye, influenced by the better exposed type Yüksekova area. Sources: Perinçek (1978, 1990), MTA (2002, 2011, 2007a,b); Robertson et al. (2026).

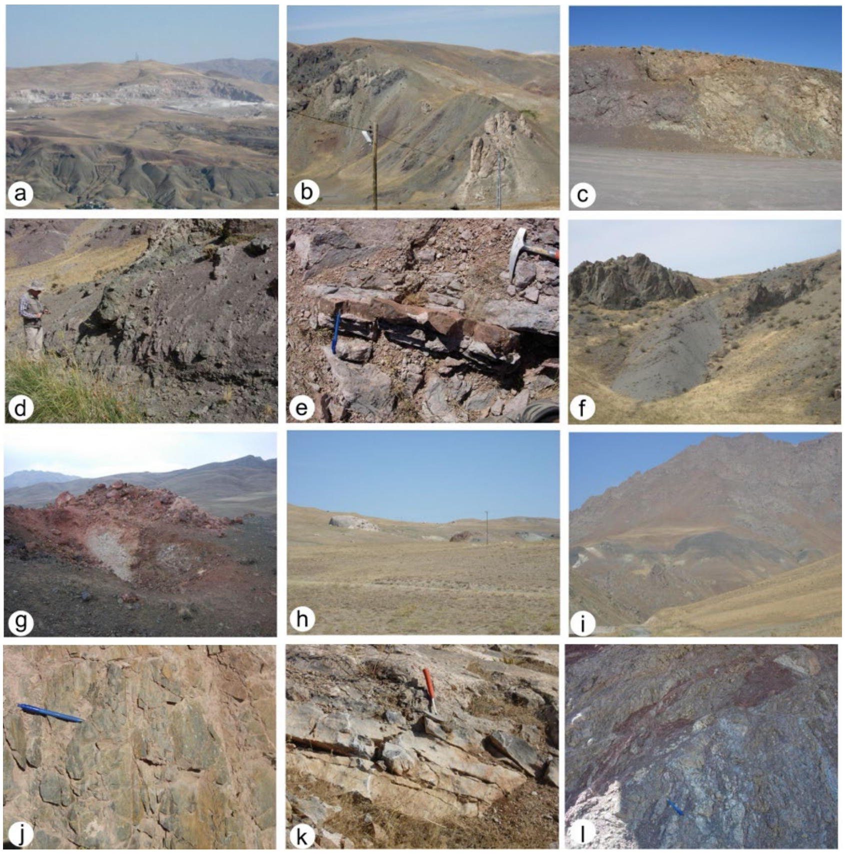

Fig. 6. Field photographs. (a) View NW from outskirts of Van city over U. Cretaceous Yüksekova Complex (grey, gently NW dipping) to Upper Palaeocene-Lower Eocene shallow-water limestone and dolomite (white; also gently dipping); (b) Upper Cretaceous Yüksekova Complex. Sheared but continuous succession of mainly basic-intermediate-composition volcanics (grey), with lenticular intercalations of pelagic limestones (white); E of Lake Erçek (5 km before turning to Satıbey); GPS; near 38S 371400E/4282634N; (c) Upper Cretaceous Yüksekova Complex; basaltic pillow lavas locally overlain by andesitic lava (E dipping; pale); 3 km S of Lake Erçek; GPS: 38S 376871E/4267145N; (d) Upper Cretaceous Yüksekova Complex; basaltic breccia (mass-flow deposit); 3 km W of Gölardı; GPS: 38S 370178E/4254752N; (e) Upper Cretaceous Yüksekova Complex. Inter-lava pink pelagic limestone with bedding-parallel layers of chert (red) formed by diagenetic replacement; c. 3 km S of Lake Erçek; GPS: 38S 377777E/4267883N; (f) Upper Cretaceous Yüksekova Complex. Volcaniclastic sandstones and mudstones (turbidites) (up to c. 10 m thick), intercalated with lava flows; 1 km E of Satıbey (c. 1 km W of Lake Erçek); GPS: 38S 370055E/4283911N; (g) Upper Cretaceous Yüksekova Complex. Minor granitic intrusion with adjacent hydrothermal alteration of lava (reddish) including disseminated copper; near Çardak; GPS: 38S 418373E/4263834N; see Figs. 2 & 7; (h) Ophiolite-related melange (low-relief) with blocks of pelagic limestone (white) and basic ophiolitic rocks in a matrix of sheared serpentinite; 2 km NE of Meydancık, N of Lake Erçek); GPS near 38S 368623E/4273999N; (i) Upper Cretaceous Yüksekova Complex (Erendağı); underlain by intersheared serpentinite (dark grey) and Yüksekova Complex lava beneath (left of road); c. 5 km SE of Van; GPS: near 38S 368916E/4254855N; (j) Felsic lava (alkaline; see Supplementary table 2), correlated with rifted Triassic platform succession of the Palaeozoic-Mesozoic unit; 2.2 km NW of Lake Erçek, GPS: 38S 379749E/4289900N; (k) Dark coloured recrystallised limestone (marble) with scattered diagenetic chert nodules; Palaeozoic-Mesozoic unit (mapped as Çomaklı Formation); 2.5 km NW of Lake Erçek, GPS: 38S 381624E/4288853N; (l) Upper Cretaceous Yüksekova Complex; altered lava with high-angle shears cut by lower angle shears; c. 4 km S of Lake Erçek (W of Lake Gövelek); GPS: 38S 376791E/4267408N.

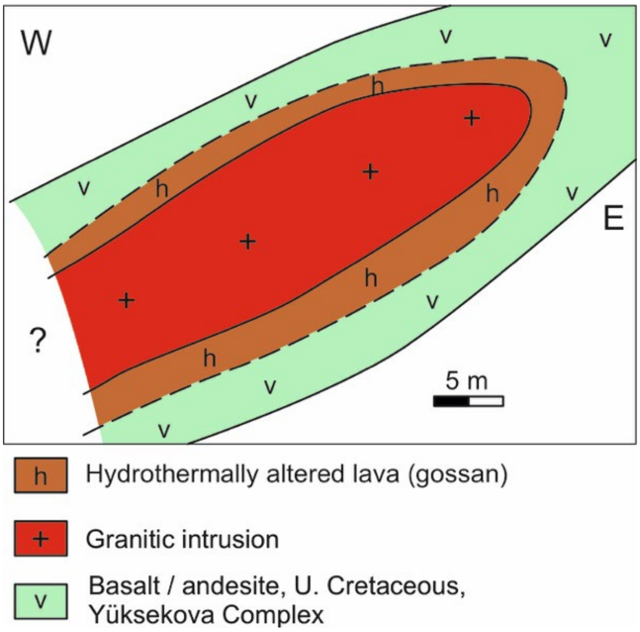

Fig. 7. Local sketch map showing the setting of disseminated copper within hydrothermally altered basaltic/andesitic lava, intruded by granite. Near Çardak; see Fig. 2. for location.

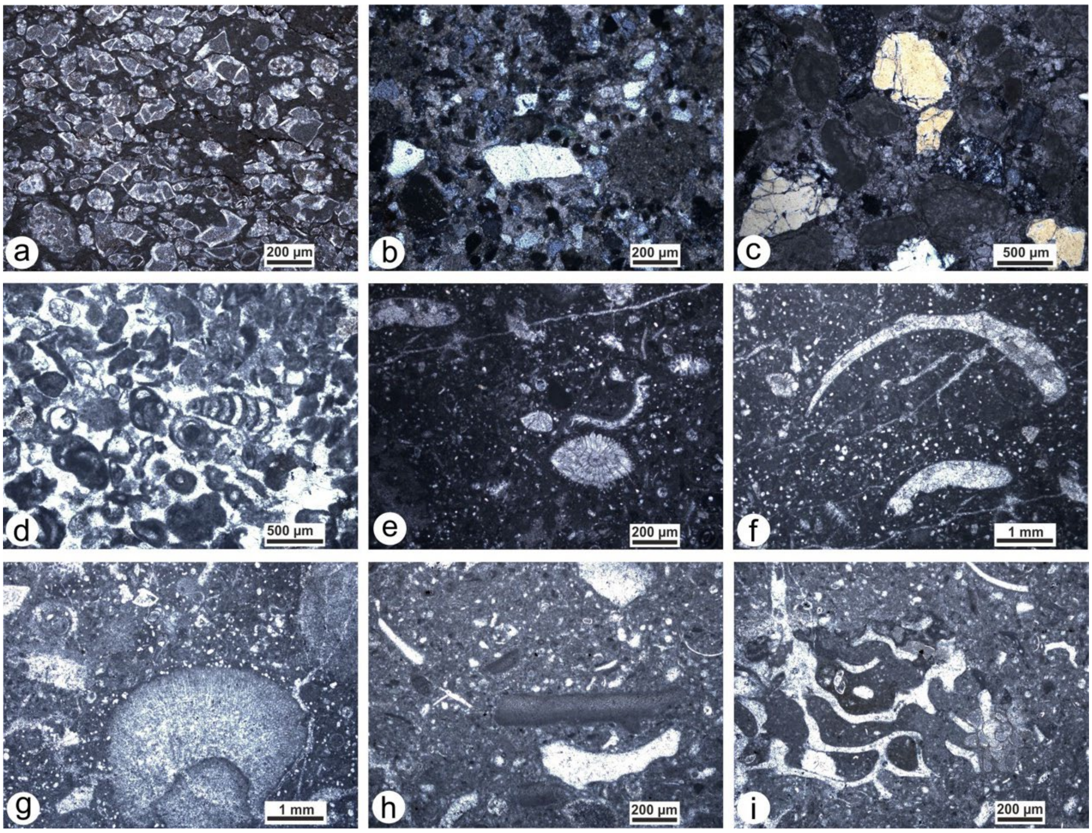

Fig. 8. Photomicrographs of the Upper Cretaceous Yüksekova Complex, the Palaeogene Seske Formation and the Oligocene-Miocene Kırkgeçit Formation, east of Lake Van. (a) Interlava pink pelagic limestones packed with planktic foraminifera (late Maastrichtian; see Supplementary Table 1), including *Globotruncana sp*.; crossed polars; Erçek-Özalp road; GPS: 38S 398452E/4279856; (b) Angular unstrained quartz crystals of volcanic origin, together with grains of glassy basalt (lower left), calcareous silt (right of large quartz grain) and plagioclase (grey); crossed polars; 1 km E of Satıbey, NE of Lake Erçek; GPS: 38S 370055E/4283911; (c) Calcareous sandstone from near the base of the cover succession (dated generally as Palaeocene-Eocene). Angular, fragmented monocrystalline quartz grains (yellow/white), together with micritic bioclasts (dark, subrounded); crossed polars; from thick-bedded mixed carbonate-siliciclastic deposit near base of cover succession; SW shore of Lake Erçek; GPS: 38S 372767E/4275043N; (d) Bioclastic platform carbonate (packstone). Benthic foraminifera in a micritic matrix (partly dissolved and replaced by calcite spar); plane-polarised light; Late Palaeocene; c. 3 km NE of Van city; GPS: 38S 360984E/4265029N; (e) Bioclastic platform carbonate (biomicrite) with benthic foraminifera; Late Palaeocene; crossed polars; c. 1 km NE Akgöl; GPS: 38S 408337E/4260776N; (f) As (e) with bivalve fragments, dissolved and infilled with calcite spar; (g) As (e) with calcareous algae (lower central) and scattered benthic foraminifera (upper); (h) Bioclastic platform carbonate (biomicrite), rich in calcareous algal fragments (central); bivalve shells (aragonitic) are dissolved and infilled with calcite spar (e.g., lower); plane-polarised light; Palaeocene-Eocene; 1 km near Bağrıaçık, W of Özalp; GPS: 38S 407515E/4264102N; (i) Biomicrite rich in fragmented calcareous algae; plane-polarised light; same location as h.

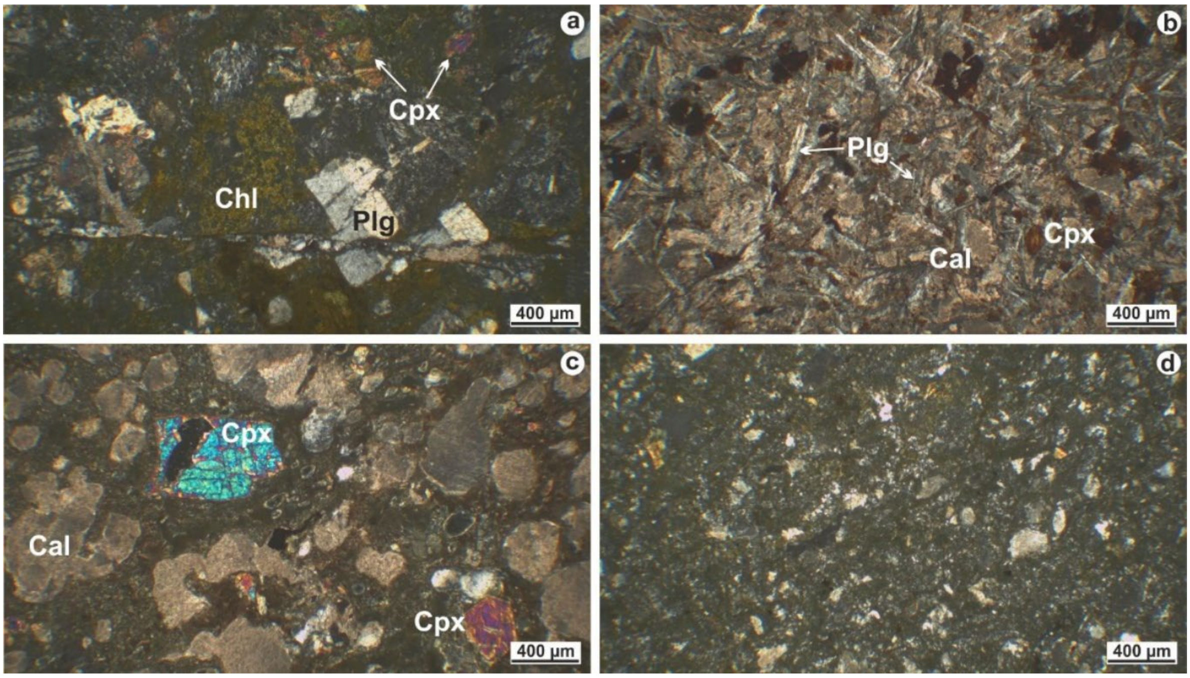

Fig. 9. Representative photomicrographs of basaltic rocks from the Van area. (a) Clinopyroxene (Cpx) and plagioclase (Plg) phenocrysts (euhedral to subhedral) with secondary chlorite (Chl); (b) Clinopyroxene and plagioclase microphenocrysts in a groundmass strongly altered to calcite (Cal); (c) Euhedral clinopyroxene phenocrysts with small amygdales infilled by calcite; (d) Finely crystalline texture, with plagioclase microlites and rare clinopyroxene microphenocrysts, with incipient calcite replacement.

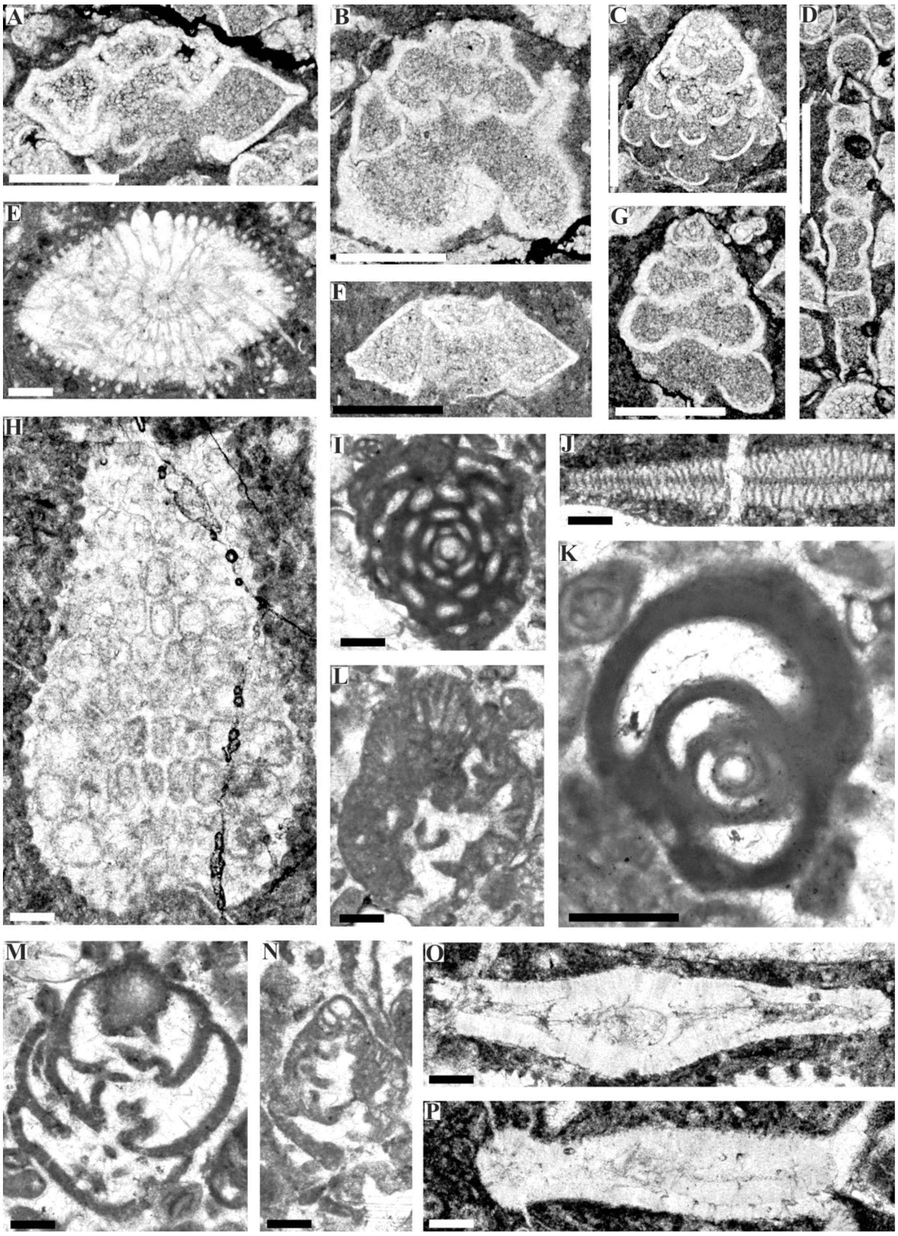

Fig. 10. Maastrichtian planktonic foraminifera*: (*A) *Globotruncanita stuarti*, Sample YU24-106; (B) *Contusotruncana contusa*, Sample YU24-106; (C, D) *Planoglobulina acervulinoides*, Sample YU24-106; (F) *Globotruncana falsostuarti*, Sample YU24-131; (G) *Planoglobulina carseyae*, Sample YU24-106. *Palaeocene benthic foraminifera and algae*; (E) *Miscellanea miscella*, Sample YU24-112; (H) *Neomeris* sp., Sample YU24-119; (I) *Glomalveolina primaeva*, Sample YU24-116; (J) *Hexagonocyclina cristensis*, Sample YU24-119; (K) *Haymanella* sp., Sample YU24-116; (L, N) *Anatoliella* sp., Sample YU24-116; (M) *Cribrobulimina carniolica*, Sample YU24-116; (O, P) *Ranikothalia* sp., Sample YU24-119. Bar scales: 0.25 mm. Sample locations: (A-D & G): 38S 398452E/4279856N; E: 38S 408337E/4260776N; F: 38S 370178E/4254752N; H, J,O,P: 38S 372604E/4276757N; I,K,L,N: 38S 360984E/4265029N.

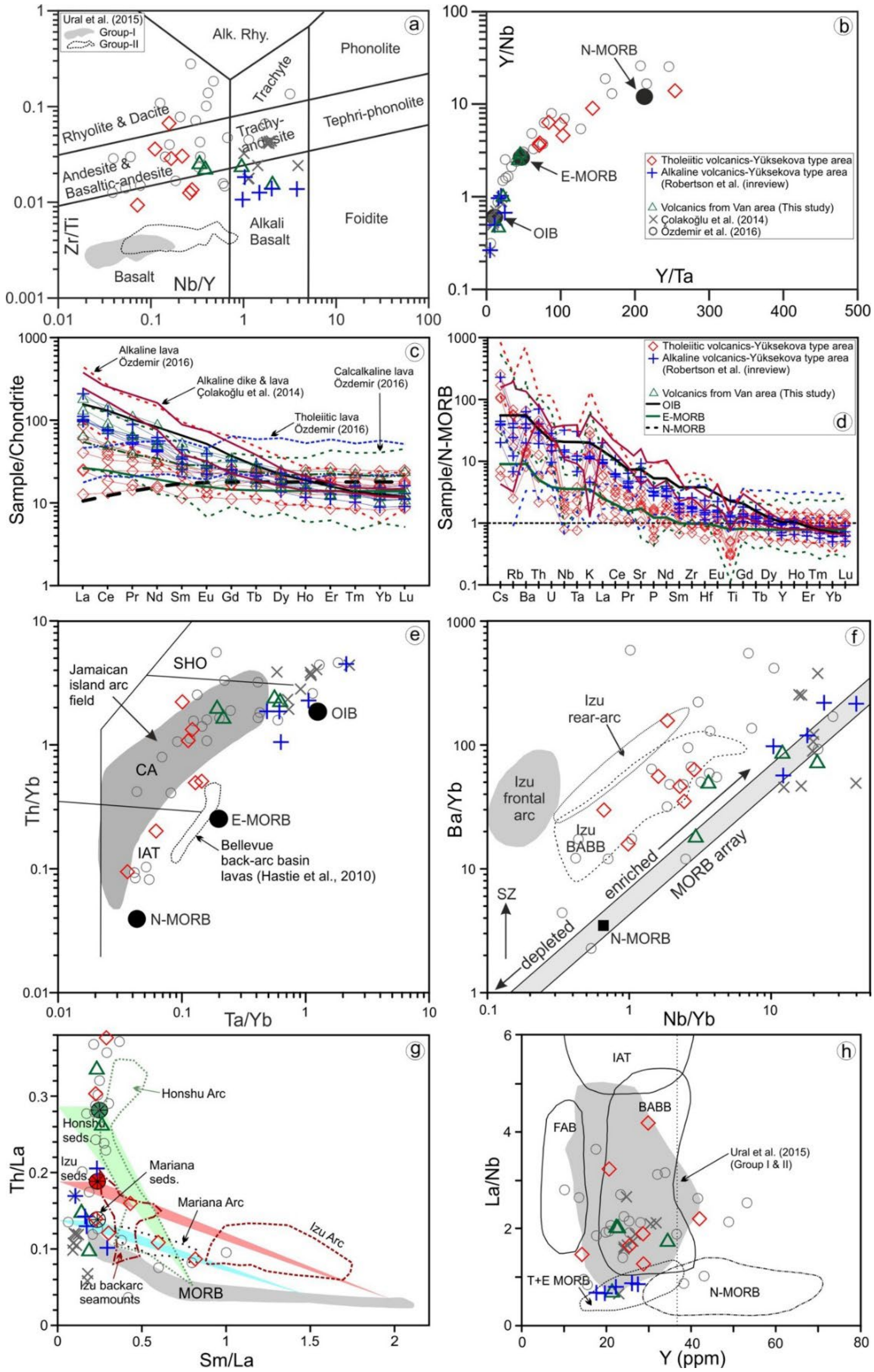

Fig. 11. Geochemistry of volcanic rocks from the Upper Cretaceous Yüksekova Complex, with modern and ancient comparisons. (a) Zr/Ti vs. Nb/Y rock classification diagram (after Pearce, 1996), (b) Mantle source characteristics of the volcanic rocks, (c) Chondrite-normalised REE diagram, (d) N-MORB normalised multi-element diagram, (e) Th/Yb vs. Ta/Yb diagram (after Pearce, 1982), (f) Ba/Yb vs. Nb/Yb diagram (after Pearce and Stern, 2006), (g) Th/La vs. Sm/La diagram (after Plank et al., 2007; arc data from Elliott et al., 1997; Gust et al., 1995; Taylor and Nesbitt, 1998 and Hochstaedter et al., 2000), and (h) La/Nb vs. Y diagram (after Floyd et al., 1991). Chondrite, N-MORB, E-MORB and OIB values from Sun and McDonough (1989); see text for explanation.

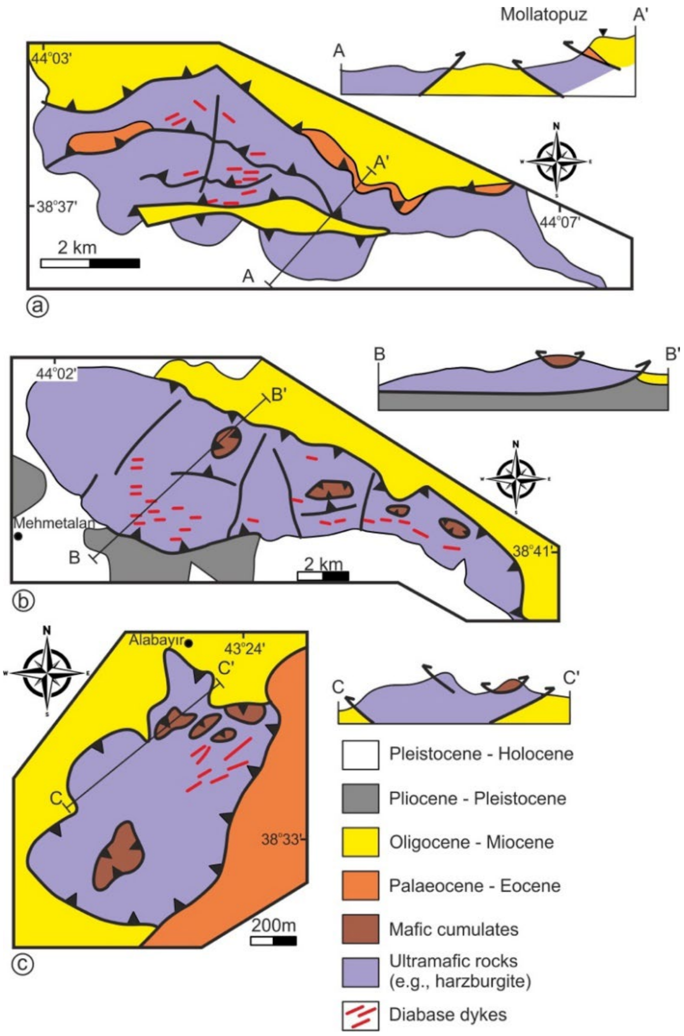

Fig. 12. Geological sketch maps and cross-sections of three significant ophiolitic bodies east of Lake Van. a, Mollatopuz; b, Mehmetalan; c, Alabayır. These fragments are dominated by mantle harzburgites, cut by isolated diabase dykes. Simplified from more detailed maps (with location grids) by Çolakoğlu et al. (2012); See Fig. 2 for locations.

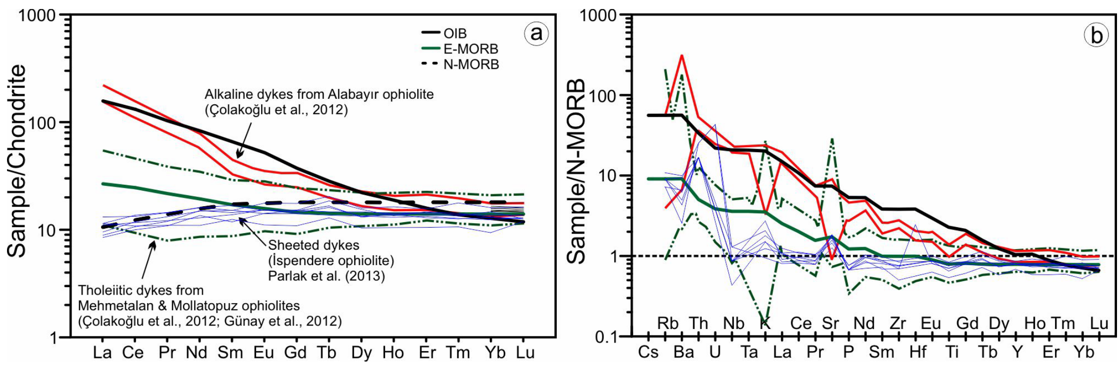

Fig. 13. Geochemistry of dykes cutting peridotites of the fragmentary Mehmetalan ophiolite exposed east of Lake Van. (a) sample/chondrite vs. REEs; (b) Sample/N-MORB vs. selected elements. N-MORB, E-MORB and OIB values are from Sun and McDonough (1989); see text for explanation.

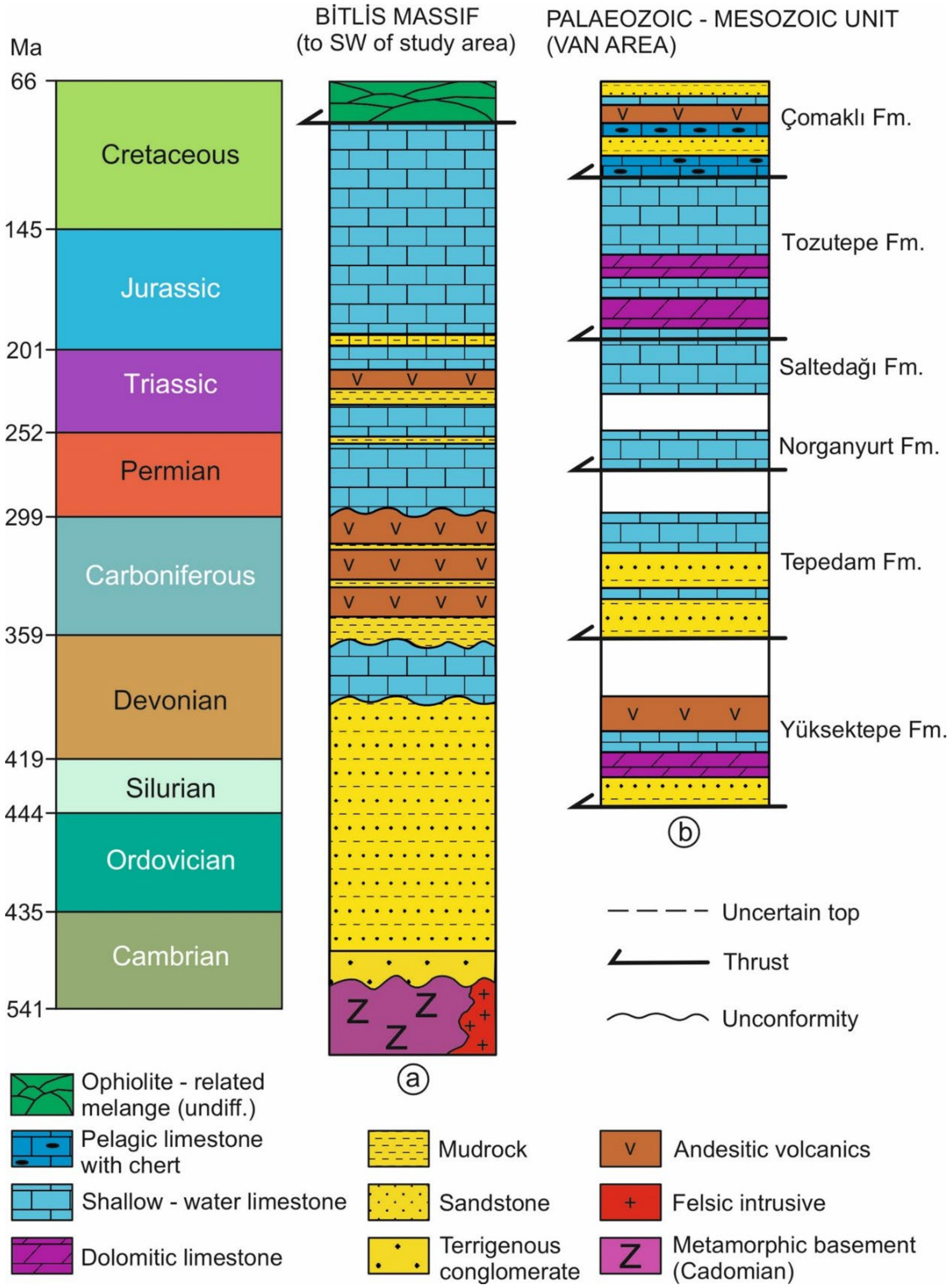

Fig. 14. Summary stratigraphic column of: (a) Bitlis Massif, simplified from Göncüoğlu and Turhan (1983), Denayer and Hoşgör (2021) and MTA (2011). (b) Palaeozoic-Mesozoic unit, as exposed east of Lake Van. Simplified from Sümengen (2008a,b,c). Note the differences especially the restriction of Cretaceous igneous rocks to the Palaeozoic-Mesozoic unit.

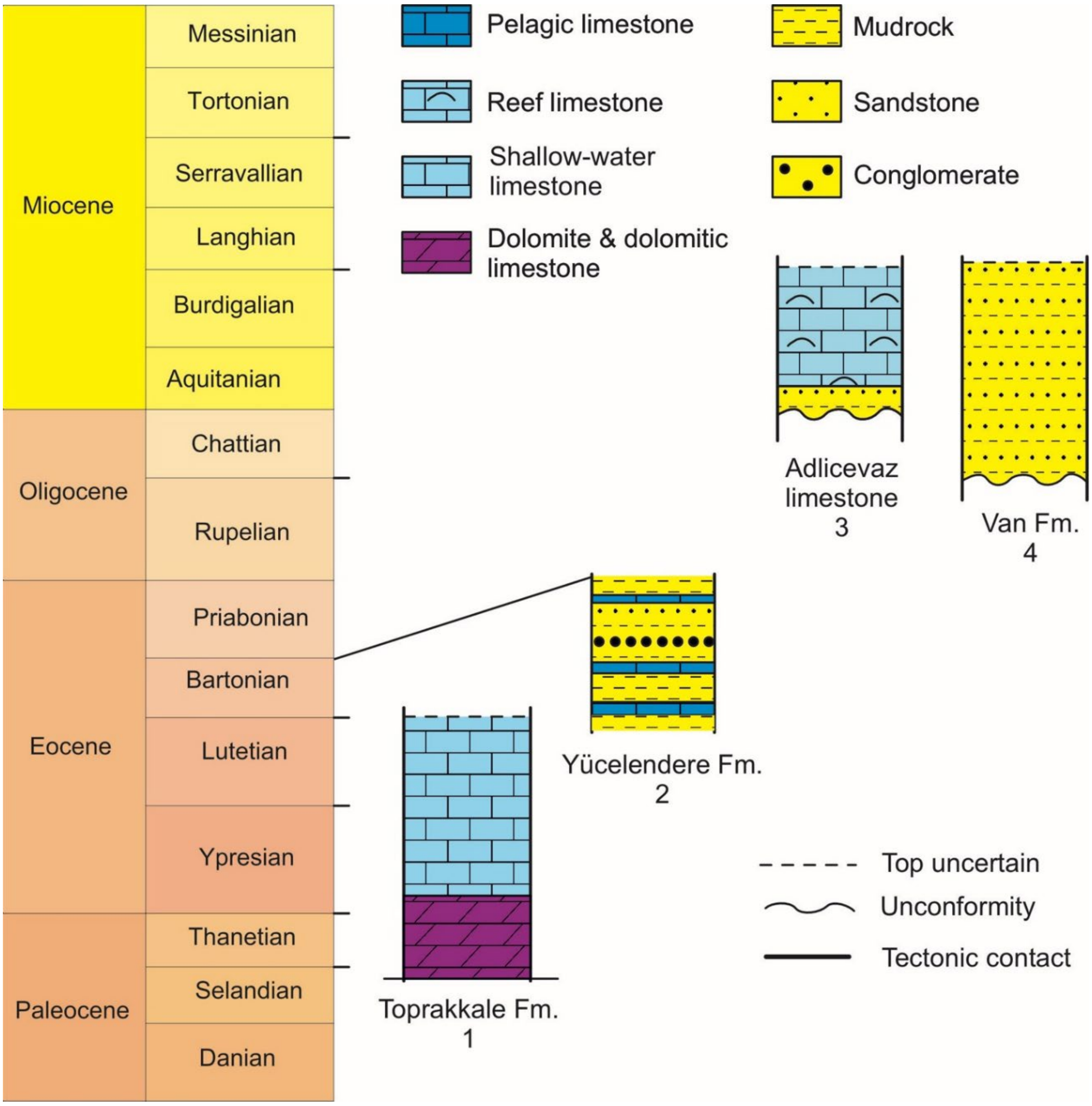

Fig. 15. Summary logs of the Palaeocene to Lower Miocene sedimentary rocks exposed in the area east of Lake Van. Data sources: Sümengen (2008 a,b,c), MTA (2011) and this study.

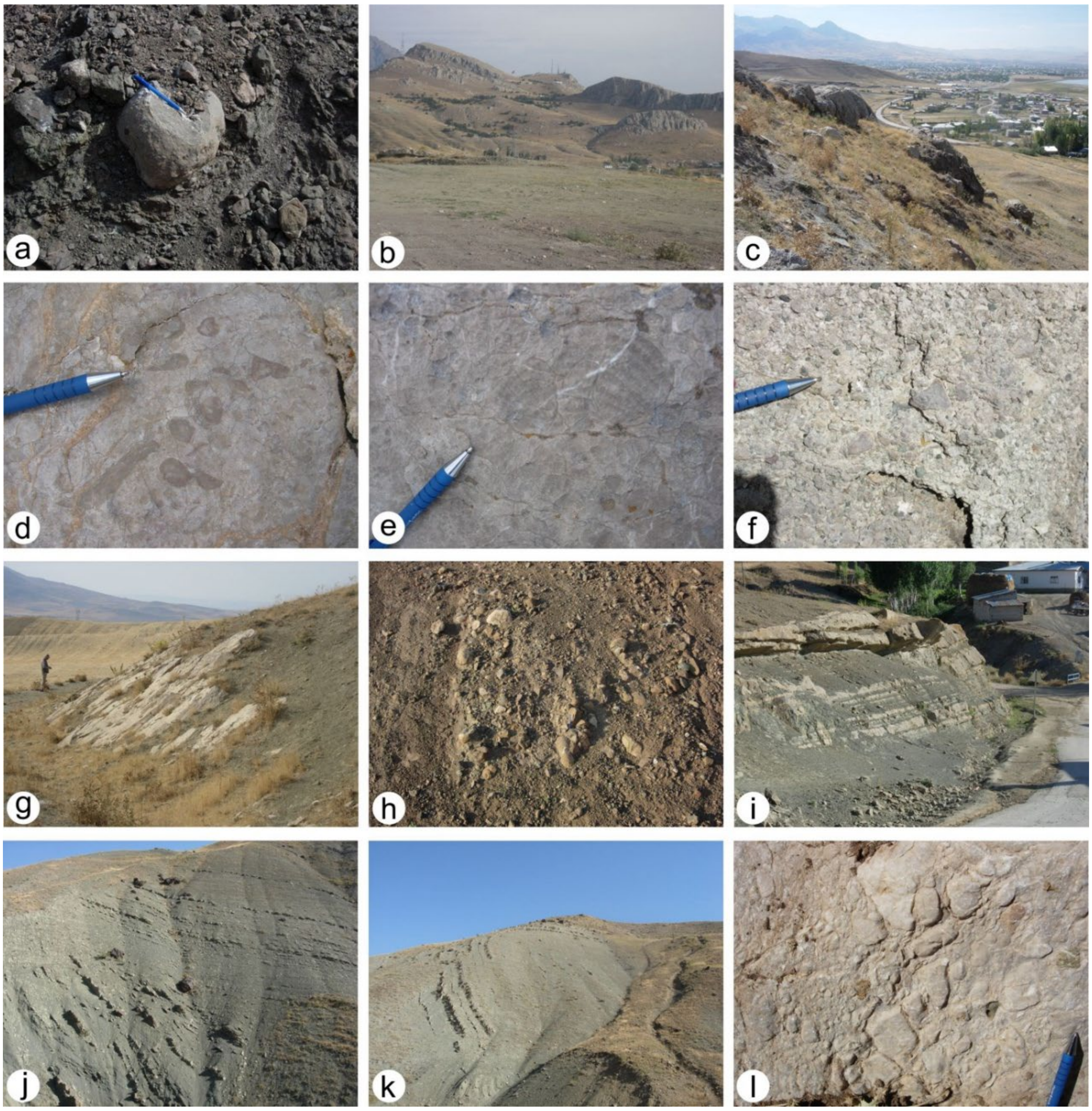

Fig. 16. Photographs of Cenozoic sedimentary facies. (a) Clast of neritic limestone (YU24-128) containing shallow-marine Bacinellid-oncoid and Verneuilinidae (agglutinated benthic foraminifer), within reworked basaltic breccia derived from the Yüksekova Complex; 3 km W of Gölardı; GPS: 38S 370178E/4254752N; (b) Palaeocene-Eocene cover, underlain by ophiolite-related melange and Yüksekova Complex volcanics (poorly exposed); view SW from 3 km NE of Van; (c) Lavas and pelagic limestones of the Yüksekova Complex (E dipping), overlain by Palaeocene-Eocene neritic limestone (W dipping; with a sheared contact), c. 2 km NE of Van; GPS: 38S 363191E/4268055N; (d) Palaeocene-Eocene neritic limestone, with oncoids, near Bağrıaçık, 2 km NE of Akgöl; GPS: 38S 407515E/4264102N; (e) Clast of calcareous algae in limestone conglomerate; location as c); (f) Middle-Late Eocene, microconglomerate including sub-rounded to sub-angular clasts of limestone and basalt; main source is Yüksekova Complex; SE shore of Lake Erçek; GPS: 38S 372767E/4275043N; (g) Well-lithified calcarenite, rich in large foraminifera, overlain by Oligocene-Miocene soft-weathering sandstone, siltstone and mudstone c. 4 km SW Kasımoğlu; GPS: 38S 357863E/4277304N; (h) Oligocene-Miocene lenticular conglomerate (60m thick) within sandstone and siltstone; well-rounded clasts include Eocene limestone, ophiolitic rocks and chert; E edge of outcrop of Oligo-Miocene (overthrust by ophiolitic melange; see Fig. 19f); c. 1km E of Arıtoprak; GPS: 38S 395435E/4266931N; (i) Oligocene-Miocene soft-weathering siltstone and mudstone; near Ortanca, c. 22 SE of Lake Erçek; GPS near 38S 395435E/4266931N; (j) Oligo-Miocene thin to medium-bedded sandstone turbidites with background siltstone/mudstone; note the intraformational unconformity; 4 km W of Gölardı; GPS: 38S 365576E/4254812N; (k) ENE-WSW verging open fold in the above sequence; same locality, field of view c. 60 m; (l) Oligocene-Miocene microconglomerate with limestone clasts containing Eocene benthic foraminifera and scattered basalt, pelagic limestone and chert clasts; near Gövelek, c. 20 km SE of Lake Erçek; GPS: 38S 380376E/4265971N.

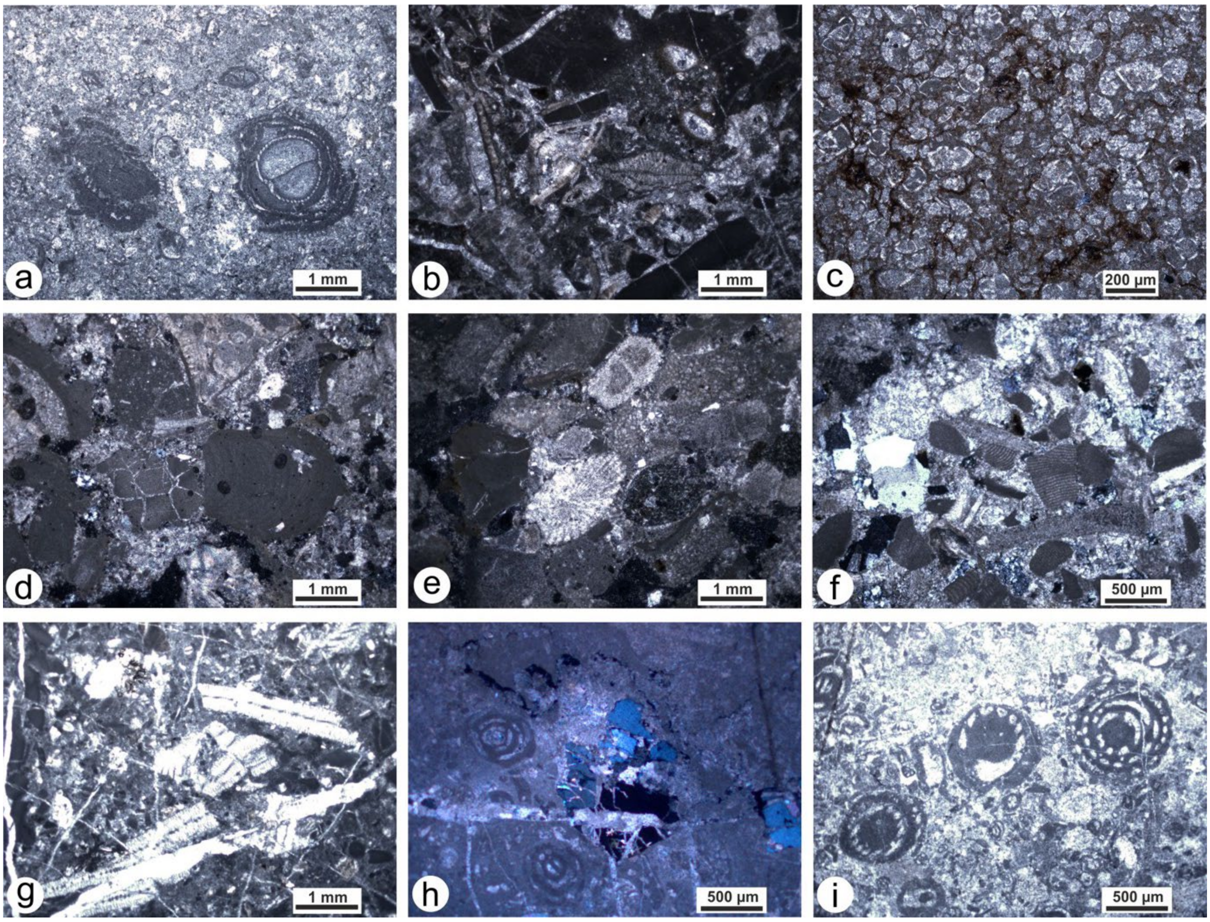

Fig. 17. Photomicrographs of Palaeocene-Eocene to Miocene sedimentary facies. (a) Biomicrite with alveolinids and silt-sized bioclastic grains (partly recrystallised to microspar); plane-polarised light; Eocene; 2 km W of Gölardı; GPS: near 38S 370888E/4254100N; (b) Biomicrite including *Discocyclina* sp. (central); numerous tectonic veins are filled with calcite spar; crossed polars; different sample from same locality as (a); (c), Pelagic limestone packed with planktic foraminifera; crossed polars; Lutetian; near Meydancık, N of Lake Erçek; GPS: 38S 374088/4290817N; (d) Shallow-water bioclastic calcarenite packed with fragments of calcareous algae; crossed polars; Oligocene-Miocene; Yeniköşk-Satıköy new road; GPS: 38S 357863E/4277304N; (e) Shallow-water bioclastic calcarenite with echinoderm spine (centre left); rounded grain of glassy basalt (centre right), micritic and algal grains; crossed polars; same location as (d); (f) Mixed carbonate-siliciclastic arenite (calcareous sandstone); poorly sorted; rich in angular fragments of calcareous algae and quartz (both monocrystalline (volcanic) and polycrystalline (metamorphic); from sandstone turbidite near the base of transgressive succession; Miocene; crossed polars; 3.5 km W of Gölardı; GPS: 38S 365576E/4254812N; (g) Biomicrite with broken *Operculina* sp.; tectonic veins; plane-polarised light; Eocene; from rounded boulder at base of transgressive Oligocene-Miocene succession; 2 km W of Gölardı; see Fig. 16a; GPS: 38S 370178E/4254752N; (h) Biomicrite with fragmented quartz vein and alveolinid benthic foraminifera (left), cut by tectonically formed and infilled calcite veins; crossed polars; Eocene (reworked); from debris-flow deposit in lower part of Oligocene-Miocene succession; c. 3 km E of Lake Gövelek; GPS: 38S 380376E/4265971N; (i) Biomicrite with alveolinids (middle) and miliolid (above right) in a micritic matrix, partly recrystallised to calcite spar; hillside east of Gövelek; GPS: 38S 380396E/4265746N.

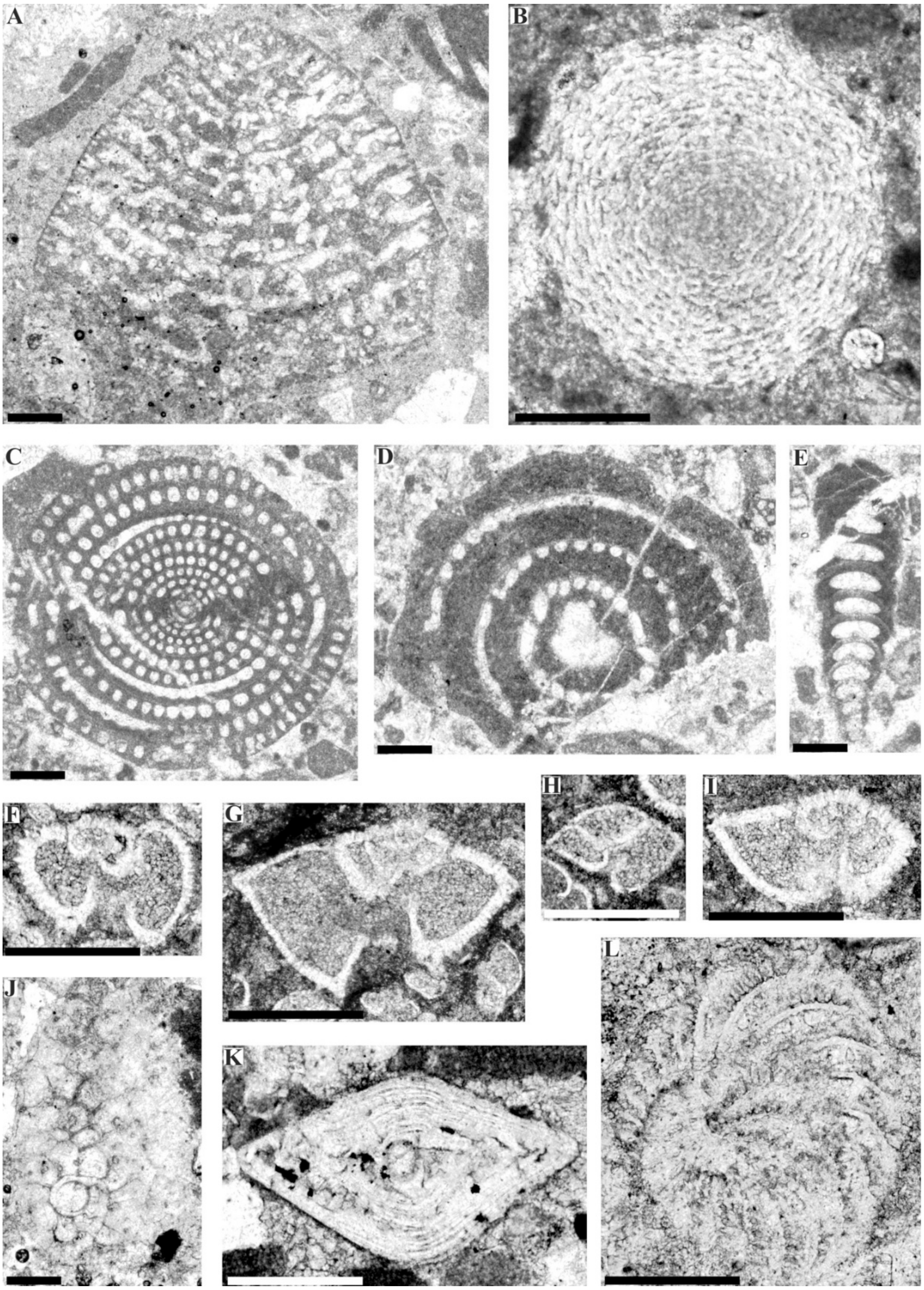

Fig. 18. Eocene benthic and planktonic foraminifera: (A) *Dictyoconus* sp., Sample YU24-94; (B) *Sphaerogypsina globula*, Sample YU24-94; (C) *Glomalveolina* sp., Sample YU24-94; (D) *Alveolina* sp., Sample YU24-94; (E) *Praerhapydionina delicata*, YU24-94; (F) *Acarinina bullbrooki*, Sample YU24-105; (G) *Morozovelloides crassatus*, Sample YU24-105; (H) *Pearsonites broedermanni*, Sample YU24-105; (I) *Acarinina praetopilensis*, Sample YU24-105. Miocene benthic foraminifera: (J) *Miogypsinoides* sp., Sample YU24-122; (K) *Amphistegina* sp., Sample YU24-123; (L) *Elphidium* sp., Sample YU24-123. Bar scales: 0.25 mm. GPS 38S (A-E): YU24-94, 380376E/4265971N; (F-I): YU24-105, 374580E 4290033N; (J): YU24-122, 357863E/4277304N; (K-L) YU24-123, 365576E/4254812N.

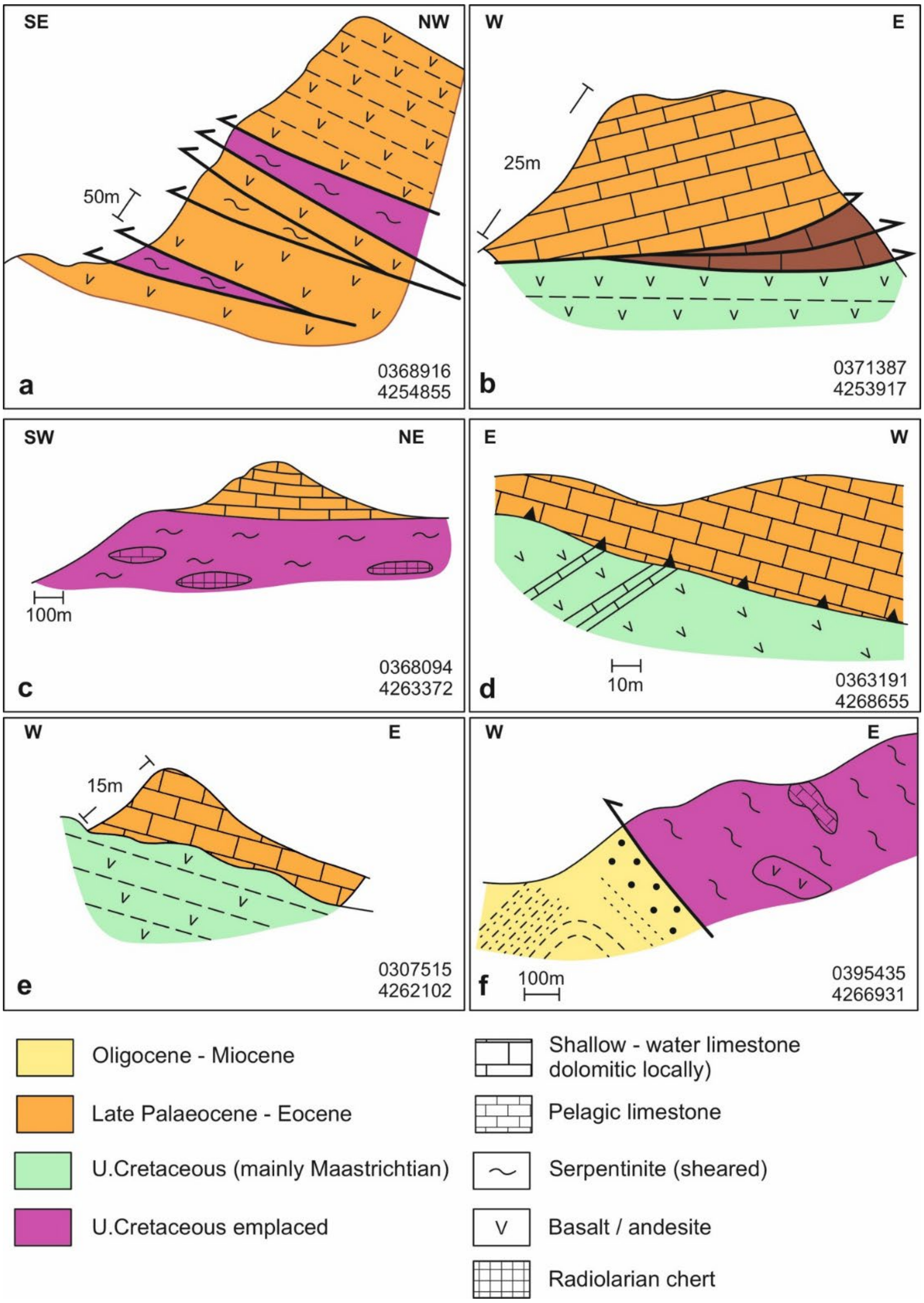

Fig. 19. Local cross-sections of key structural features east of Lake Van; see Fig. 2 for locations. (a) Serpentinised harzburgite intersliced with Yüksekova Complex lava; SW margin of Erekdağı; (b) Palaeocene neritic lava overlying Upper Cretaceous Yüksekova Complex lava with a sheared contact; c. 2 km W of Gölardı; (c) Ophiolite-related melange with blocks of radiolarite and pelagic limestone in a matrix of sheared serpentinite, overlain (with a normal contact) by Upper Palaeocene shallow-water limestones; 3 km E of Van city; (d) Lava with pelagic limestone interbeds of the Yüksekova Complex, with Palaeocene neritic limestones thrust above; the contact truncates the bedding in the Yüksekova Complex and shows evidence of tectonic brecciation along the contact; c. 2 km NW of Lake Bostaniçi, NE of Van city; (e) Lavas of the Yüksekova Complex unconformably overlain by Palaeocene-Eocene neritic limestone; near Bağrıaçık; south central area; (f) Ophiolite-related melange locally thrust over Oligo-Miocene succession (folded) with lenticular conglomerates near the base; c. 2 km NE of Dereköy.

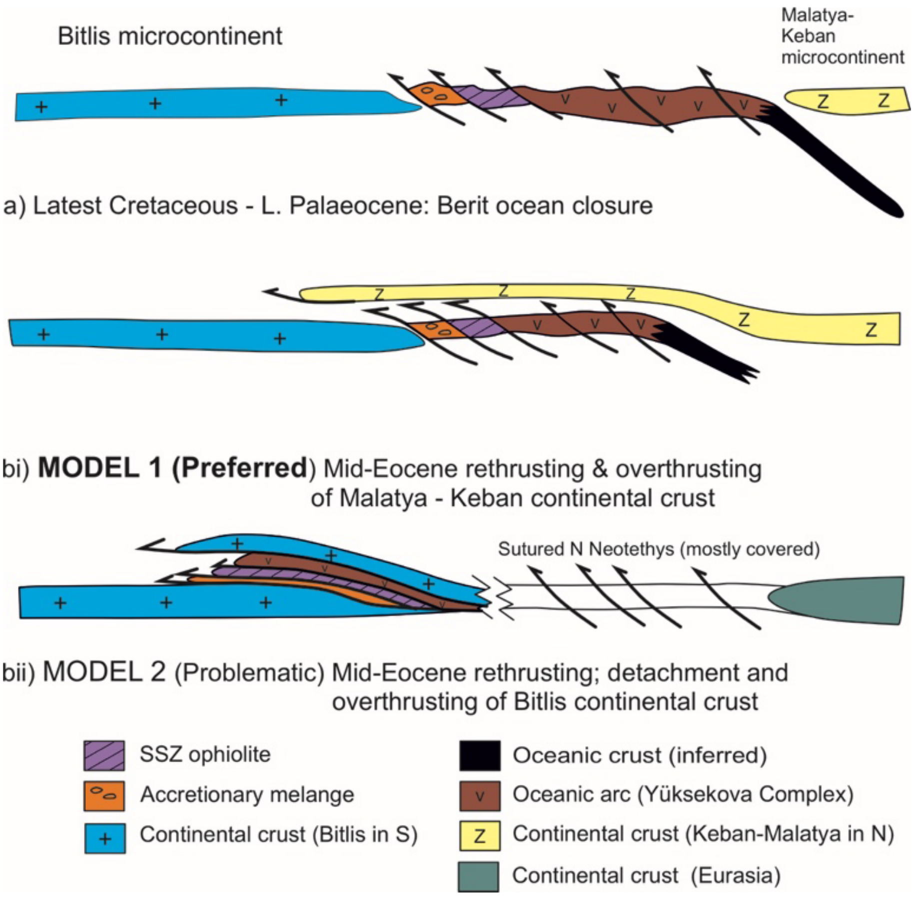

Fig. 20. Emplacement of tectonic units in the study area east of Lake Van. (a) initial latest Cretaceous-Early Palaeocene(?) emplacement as an accretionary complex; (bi-ii) later stage, Eocene rethrusting; (bi) assumes correlation of the Palaeozoic-Mesozoic unit with the Malatya-Keban platform farther west, with southward high-level overthrusting; (bii) assumes correlation of the Palaeozoic-Mesozoic unit with the Bitlis Massif to the southwest which would require thick-skinned southward rethrusting; (bi) is preferred (see text).

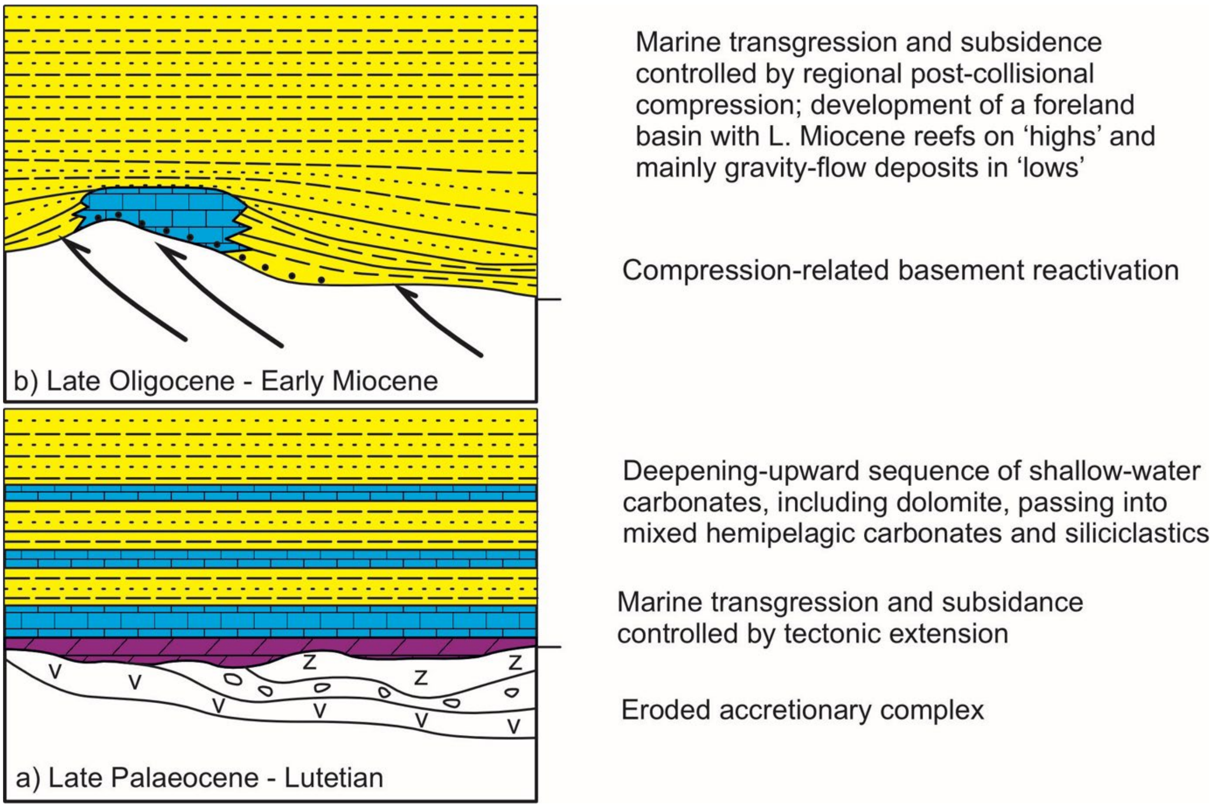

Fig. 21. Summary and interpretation of the Upper Cretaceous to Miocene successions to the east of Lake Van; (a) late Palaeocene-Middle Eocene (Lutetian) inferred extensional setting; (b) late Oligocene-Early Miocene inferred compressional setting (see Fig. 15 for more detailed sedimentary logs).

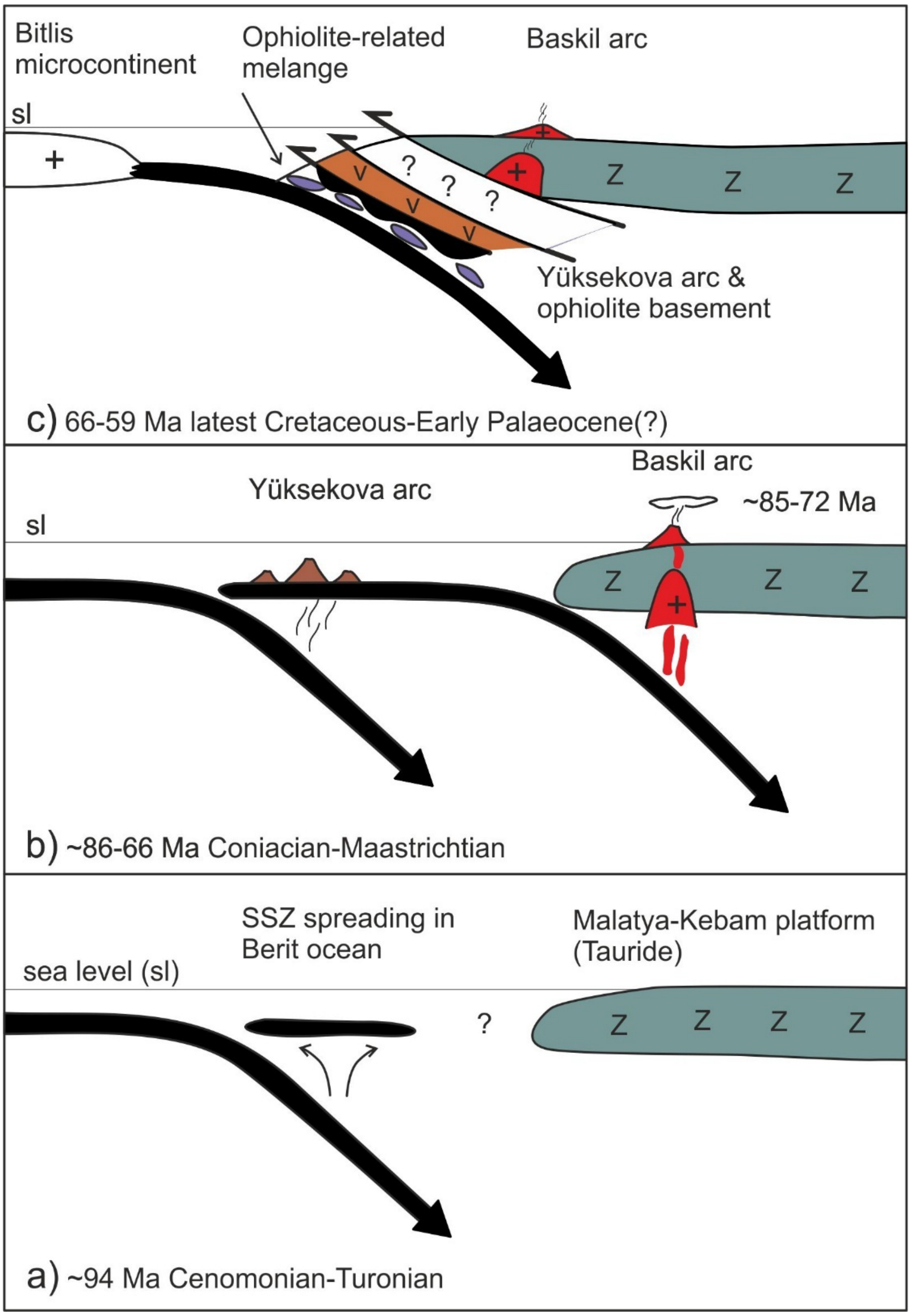

Fig. 22. Tectonic model for the Late Cretaceous development of the Berit Suture Zone in its type area farther west (see Fig. 1); this is broadly applicable to the present study area east of Lake Van. (a) Supra-subduction spreading formed future ophiolites (an unknown distance from the Tauride microcontinent to the north); (b) further subduction initiated the intra-oceanic Yüksekova volcanic arc. Northward subduction beneath the Tauride microcontinent simultaneously generated the intra-continental Baskil arc; (c) during continuing subduction, ophiolitic units and the Yüksekova arc accreted and were emplaced over the Bitlis-Pütürge continental fragments to the south (see Fig. 14a). The study area differs from the type are of the Berit Suture Zone mainly because of the absence of exposed Bitlis-type crust in the south, longer distance southward emplacement, and more complex and variable multi-stage deformation.

Table S1 - Foraminifera and calcareous algae identified east of Van Lake

Sample no.	*Microfossils*	*Age*
YU24-91 red	*Globotruncana arca*, *G. linneiana*, *G. falsostuarti* Sigal 1952, *G. ventricosa* (White) 1928	late Campanian-Maastrichtian
YU24-100 red	*Globotruncanita stuarti*, *Planoglobulina carseyae*, *Pseudotextularia elegans*	late Campanian -Maastrichtian
YU24-106 red	*Contusotruncana contusa*, *Globotruncanita stuarti*, *Planoglobulina carseyae*, *Planoglobulina* cf. *P. acervulinoides*, *Planohedbergella subcarinata*, *Pseudotextularia elegans*	late Maastrichtian
YU24-113 red	*Contusotruncana fornicata*, *Globotruncana falsostuarti*, *Planoglobulina* cf. *P. acervulinoides*, *Pseudotextularia elegans*	late Campanian-Maastrichtian
YU24-131 red	*Globotruncana bulloides*, *G. falsostuarti*, *Pseudotextularia elegans* (Rzehak) 1891, *Planoglobulina* cf. *P. acervulinoides* (Egger) 1902	late Campanian-Maastrichtian
YU24-112	*Miscellanea miscella* (d'Archiac and Haime) 1853, *Rotalia* sp., Miliolidae, Halimeda sp., dasycladalean alga, coralline algae	Palaeocene
YU24-116	*Glomalveolina primaeva* (Reichel) 1936, *Cribrobulimina carniolica* Hottinger and Drobne 1980, *Haymanella* sp., *Anatoliella* sp., *Rotorbinella* sp.	Late Palaeocene
YU24-118	sandstone *Kayseriella*? sp. (reworked), Rotaliidae	Palaeocene?-Eocene
YU24-119	*Hexagonocyclina cristensis* (Vaughan) 1924, *Hottingerina* sp., *Kathina* sp., *Ranikothalia* sp., *Cymopolia* sp., *Neomeris* sp.,	Late Palaeocene
YU24-109	*Planorbulina* sp., *Valvulina* sp., *Biloculina* sp., dasycladalean alga, coralline alga	Palaeocene-Eocene?
YU24-94	*Dictyoconus* sp., *Alveolina* sp., *Glomalveolina* sp., *Sphaerogypsina globula* (Reuss) 1848, *Idalina sinjarica* Grimsdale 1952, *Praerhapydionina delicata* Henson 1950, *Rotalia* sp.	Eocene
YU24-129	*Asterigerina rotula* (Kaufmann) 1867, *Sphaerogypsina globula* (Reuss) 1848 *Discocyclina* sp., *Nummulites* sp., *Rotalia* sp.	Eocene
YU24-124	*Asterigerina rotula* (Kaufmann) 1867, *Gyroidinella* sp., *Asterocyclina sp., Discocyclina* sp., *Nummulites* sp.	Eocene
YU24-125	*Assilina* sp., *Nummulites* sp., *Glomalveolina lepidula*, *Alveolina* spp., *Orbitolites* sp., Rotalidae	Eocene

YU24-105 red	*Acarinina bullbrooki* Bolli 1957, *A. praetopilensis* (Blow) 1979, *Morozovelloides crassatus* (Cushman) 1925, *Pearsonites broedermanni* (Cushman and Bermudez) 1949	Lutetian
YU24-122	*Miogypsinoides* sp., *Victoriella* sp., sponge, coralline alga, bryozoa, echinoderm	Oligocene-Miocene
YU24-123	*Amphistegina* sp., *Miogypsinoides* sp., *Elphidium* sp., Globigerinidae, sponge, coralline alga,	Miocene

Locations of samples: GPS 38S YU24-91, 377777E/4267883N; YU24-100, 378989E/4290284N; YU24-106, 38452E/4279856N; YU23-113, 410780E/4257708N; YU23-131, 370178E/4254752N; YU23-112, 38337E/4260776N; YU23-116, 360984E/4265029N; YU23-118, 3727667E/4275043N; YU23-119, 372604E/4276757N; YU23-109, 407515E/4264102N; YU24-94, 380376E/4265971N; YU24-129, 370178E/4254752N; YU24-124, 125, 370888E/4254100N; YU24-105, 374580E/4290033N; YU24-122, 357863E/4277304N; YU24-123, 365576E/4254812N.

Table S2 - Major, trace and rare earth element data for representative volcanic rocks from the study area east of Lake Van

	Tholeiitic		Alkaline		Palaeozoic-Mesozoic unit
	Pillow lava		Pillow lava		Alkaline lava
	38S 376871E/4267145N	38S 370178E/4254752N	38S 378989E/4290284N	38S 398452E/4279856N	38S 379749E/4289900N
Sample No	**YU24-87**	**YU24-130**	**YU24-103**	**YU24-115**	**YU24-97**
SiO_2	53	55.2	40.8	34.2	59.44
TiO_2	1.3	0.85	1.27	0.96	0.80
Al_2O_3	16.8	16.35	15.3	11.2	19.92
FeO*	10.1	8.69	9.9	9.11	8.49
MgO	3.52	3.67	4.25	7.83	4.19
MnO	0.21	0.11	0.25	0.15	0.05
CaO	4.56	4.38	12.6	19.4	0.52
Na_2O	4.55	6.7	4.55	1.52	0.93
K_2O	1.05	0.32	0.26	1.46	5.39
Cr_2O_3	0.009	0.003	0.045	0.07	0.01
P_2O_5	0.29	0.13	0.38	0.45	0.19
SrO	0.01	0.01	0.05	0.03	<0.01
BaO	0.02	0.01	0.02	0.02	0.07
LOI	4.34	2.83	11	13.7	4.42
Total	99.76	99.25	100.68	100.1	100.32
Ba	186.5	48	153.5	156.5	586.00
Cs	0.11	0.02	0.16	0.62	7.15
Th	6.23	5.26	4.78	4.38	14.05
Rb	20.5	5.5	5.9	38.4	153.00
Sr	155.5	107	489	339	30.50
Sc	35	23.1	28	41.4	19.80
Cr	66	23	344	533	88.00
U	1.74	1.69	0.97	0.99	3.28
V	134	222	232	199	166.00
W	1.3	1	1.1	0.5	3.40
Zr	180	134	122	141	139.00
Y	34.4	22.7	21.3	22.3	25.50
Nb	13.3	7.6	43.8	21.3	15.95
Ta	0.8	0.5	1.3	1	1.30
Hf	4.55	3.67	2.63	3.08	3.91
Ga	20.2	21.5	16.6	14.2	29.10
La	23.6	15.6	31.9	43.9	50.00
Ce	47.6	30.7	56.9	89	109.00
Pr	6.18	3.83	6.35	10.7	11.90
Nd	25.2	14.8	23.7	41.9	43.40
Sm	6.19	3.62	4.5	8.2	7.07
Eu	1.75	1.01	1.39	2.41	1.34
Gd	6.39	3.95	4.38	7.26	5.32
Tb	1.1	0.67	0.73	1	0.80
Dy	6.46	4.39	4.1	5.06	4.72
Ho	1.35	0.9	0.84	0.91	0.98
Er	4	2.68	2.15	2.05	2.92
Tm	0.59	0.41	0.34	0.33	0.41
Yb	3.69	2.59	2.08	1.78	3.03
Lu	0.62	0.38	0.33	0.28	0.46